

12-2013

# CXCR2 EXPRESSION IN TUMOR CELLS IS A POOR PROGNOSTIC FACTOR AND PROMOTES INVASION AND METASTASIS IN LUNG ADENOCARCINOMA

Erminia Massarelli

Follow this and additional works at: [http://digitalcommons.library.tmc.edu/utgsbs\\_dissertations](http://digitalcommons.library.tmc.edu/utgsbs_dissertations)

 Part of the [Medical Cell Biology Commons](#), and the [Oncology Commons](#)

---

## Recommended Citation

Massarelli, Erminia, "CXCR2 EXPRESSION IN TUMOR CELLS IS A POOR PROGNOSTIC FACTOR AND PROMOTES INVASION AND METASTASIS IN LUNG ADENOCARCINOMA" (2013). *UT GSBS Dissertations and Theses (Open Access)*. Paper 409.

This Thesis (MS) is brought to you for free and open access by the Graduate School of Biomedical Sciences at DigitalCommons@The Texas Medical Center. It has been accepted for inclusion in UT GSBS Dissertations and Theses (Open Access) by an authorized administrator of DigitalCommons@The Texas Medical Center. For more information, please contact [laurel.sanders@library.tmc.edu](mailto:laurel.sanders@library.tmc.edu).

CXCR2 EXPRESSION IN TUMOR CELLS IS A POOR PROGNOSTIC FACTOR AND  
PROMOTES INVASION AND METASTASIS IN LUNG ADENOCARCINOMA

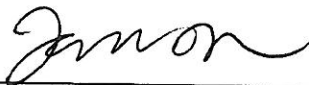
by

Erminia Massarelli, MD, PhD

APPROVED:



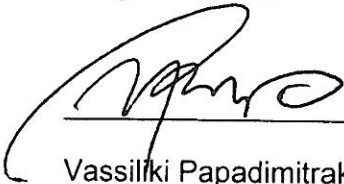
Supervisory Professor: Jonathan M. Kurie, MD



Faye M. Johnson, MD, PhD



Greg Lizee, PhD



Vassiliki Papadimitrakopoulou, MD



Ignacio I. Wistuba, MD

APPROVED:

\_\_\_\_\_  
Dean, The University of Texas

Graduate School of Biomedical Sciences at Houston

CXCR2 EXPRESSION IN TUMOR CELLS IS A POOR PROGNOSTIC FACTOR AND  
PROMOTES INVASION AND METASTASIS IN LUNG ADENOCARCINOMA

A

THESIS

Presented to the Faculty of  
The University of Texas  
Health Science Center at Houston  
and  
The University of Texas  
MD Anderson Cancer Center  
Graduate School of Biomedical Sciences  
in Partial Fulfillment

of the Requirements

for the Degree of

MASTER OF SCIENCE

by

Erminia Massarelli, MD, PhD

Houston, Texas

December 2013

## ACKNOWLEDGEMENTS

I would like to thank current and former members of Dr. Jonathan Kurie's laboratory for their help in acquiring the technical skills and for their scientific advice to perform laboratory experiments including Jonathon Roybal, PhD, Brandi N. Baird, PhD, Yanan Yang, PhD, Young-Ho Ahn, PhD.

I would like to thank Pierre Saintigny, MD, PhD for his help in the gene analysis section, Steven Lin, MD for his help in the gene methylation analysis, Ignacio I. Wistuba, MD for his help and support provided in the interpretation of the pathological results of this project and Diane Liu for her help in the biostatistical analysis.

Most of all, I would like to thank my advisor, Jonathan M. Kurie, MD and the other members of my advisory committee, Vassiliki Papadimitrakopoulou, MD, Faye Johnson, MD, PhD, Greg Lizee, MD and Ignacio I. Wistuba, MD for their guidance and support.

# CXCR2 EXPRESSION IN TUMOR CELLS IS A POOR PROGNOSTIC FACTOR AND PROMOTES INVASION AND METASTASIS IN LUNG ADENOCARCINOMA

Erminia Massarelli, MD, PhD

Supervisory Professor: Jonathan M. Kurie, MD

CXC chemokine receptor 2 (CXCR2) is a G-protein coupled receptor which mediates signaling by binding to CXC chemokines CXCL1-3 and 5-8. In non-small cell lung cancer CXCR2 has been studied mainly in stromal cells and is known to increase tumor inflammation and angiogenesis. However, there is controversial data in the literature about CXCR2 expression in tumor cells and its role in the tumor microenvironment. We hypothesized that tumoral expression of CXCR2 and its ligands promote tumor invasion and metastasis in non-small cell lung cancer.

The effect of CXCR2 expression on tumor cells was studied using stable knockdown clones derived from a murine *KRAS/p53*-mutant lung adenocarcinoma cell line (344SQ) with high metastatic potential and an orthotopic syngeneic mouse model and *in vitro* using a CXCR2 small molecule antagonist (SB225002). We showed that *in vivo* CXCR2 inhibition by knock-down reduces its invasive ability. In a murine model of orthotopic syngeneic lung adenocarcinoma CXCR2 knock-down 344SQ cell line was found to be associated with decreased tumor burden, local and distant metastases.

In order to translate our preclinical discoveries to human NSCLC, we explored CXCR2 tumoral immunohistochemical expression in 262 tissue microarrays created from tumor specimens of patients with surgically resected stage I-II lung adenocarcinoma and correlated it with patient clinic-pathological characteristics including smoking status, histological differentiation and survival outcomes. We considered also localization of CXCR2 expression in the cytoplasm, membrane and nucleus. High cytoplasmic CXCR2

was associated with smoking history, aggressive histological differentiation and worse survival. When we screened a publicly available large database of human NSCLC cell lines (N=52) and human lung adenocarcinomas (N=442), we found that at the gene expression level, *CXCL5*, a *CXCR2*-ligand, was the main driver of a cluster of cell lines and lung adenocarcinomas with high-risk features, including *RAS* and *MET* pathway activation, epithelial-to-mesenchymal transition and resistance to epidermal growth factor inhibition (i.e., gefitinib). We studied promoter methylation in 70 human non-small cell lung cancer cell lines and discovered that *CXCL5* was regulated by promoter methylation.

We concluded that the *CXCR2* axis may be an important target in smoking-related lung adenocarcinoma.

## TABLE OF CONTENTS

LIST OF FIGURES.....	Page vii
LIST OF TABLES.....	Page viii
ABBREVIATIONS.....	Page ix
INTRODUCTION.....	Page 1
MATERIAL AND METHODS.....	Page 6
RESULTS.....	Page 9
DISCUSSION.....	Page 40
BIBLIOGRAPHY.....	Page 45
VITA.....	Page 57

## LIST OF FIGURES

Figure 1. Mediastinal lymph node metastasis from an orthotopic lung tumor. ....	Page 10
Figure 2. Effect of CXCR2 downregulation and inhibition.....	Page 12
Figure 3. Distribution of cytoplasmic CXCR2 protein expression.....	Page 15
Figure 4. Expression of CXCR2 and its ligands in tumor cells and tissues.....	Page 16
Figure 5. Median CXCR-2 immunohistochemistry score.....	Page 17
Figure 6. CXCR2 expression according to <i>EGFR</i> and <i>KRAS</i> mutation status.....	Page 18
Figure 7. Overall survival and recurrence-free survival as a function of cytoplasmic CXCR2 expression in lung adenocarcinoma.....	Page 19
Figure 8. Overall survival and recurrence-free survival as a function of cytoplasmic CXCR2 expression in lung adenocarcinoma.....	Page 20
Figure 9. Distribution of expression of <i>CXCR2</i> , its ligand genes and <i>IL8</i> in non-small cell lung cancer cell lines and lung adenocarcinomas.....	Page 24
Figure 10. <i>CXCR2/CXCR2</i> ligands association with overall survival in patients with lung adenocarcinoma.....	Page 25
Figure 11. <i>TTF-1</i> gene expression in lung adenocarcinomas and cell lines.....	Page 27
Figure 12. Identification of a <i>CXCR2/CXCR2</i> ligands cluster.....	Page 29
Figure 13. Expression of <i>CXCR2</i> and its ligand genes in NSCLC cell lines.....	Page 31
Figure 14. Expression of <i>CXCR2</i> and its ligand genes in lung adenocarcinomas.....	Page 33
Figure 15. PC1 and overall survival.....	Page 34
Figure 16. CXCL5 upregulation and overall survival.....	Page 35
Figure 17. CXCL5 drives the <i>CXCR2/CXCR2</i> ligands cluster and is regulated through promoter methylation.....	Page 36
Figure 18. Promoter methylation of CXCR2 ligand genes.....	Page 38
Figure 19. Effect of decitabine on CXCR2 ligand genes.....	Page 39



## LIST OF TABLES

Table 1. Clinical and pathological characteristics of patients included in the tissue microarray.....	Page 14
Table 2. Univariate Cox model assessing the effect of covariates on overall survival and recurrence-free survival in adenocarcinoma patients.....	Page 21
Table 3. Univariate Cox model assessing the effect of covariates on overall survival and recurrence-free survival in squamous cell carcinoma patients.....	Page 22
Table 4. Final multivariate Cox models assessing the effect of covariates on overall survival in the whole population, in patients with lung adenocarcinoma and in patients with lung squamous cell carcinoma.....	Page 23

## ABBREVIATIONS

CAF=cancer associated fibroblasts

COPD= chronic obstructive pulmonary disease

DSP=desmoplakin

DUSP4=dual specific phosphatase 4

EGFR=epidermal growth factor receptor

FBS=fetal bovine serum

FOLR1=folic acid receptor 1

GEO=gene expression Omnibus

GSEA=gene set enrichment analysis

HGF=hepatocyte growth factor

HBEC=human bronchial epithelial cells

HR=hazard ratio

IHC=immunohistochemistry

IPA=ingenuity pathway analysis

MAP=mitogen-activated protein

NKX2-1=thyroid transcription factor 1

NSCLC=non small cell lung cancer

PC1=principal component

PLC=phospholipase C

RRM2=ribonucleotide reductase M2

SPP1=osteopontin

SPINT1=hepatocyte growth factor activator inhibitor 1

SFTP=surfactant protein

TGFB1=tumor growth factor B1

TMA=tissue microarray

TTF1=thyroid transcription factor-1

VEGF=vascular endothelial growth factor

VIM=vimentin

## INTRODUCTION

Lung cancer is responsible for over a million of deaths worldwide per year<sup>1</sup>. Diagnosis is often made at an advanced stage and the 5-years survival remains poor (about 15%) with only little progress in the last two decades. Lung cancer histology drives the therapeutic decisions and chemotherapy choice. Small-cell lung cancers and non-small-cell lung cancers (NSCLC) are the two major histological subtypes<sup>2</sup>. Lung adenocarcinoma, a subtype of NSCLC, represents about 50% of the total number of lung cancers. First-line chemotherapy for advanced/metastatic NSCLC consists of combination chemotherapy with platinum compounds<sup>3</sup>. In particular, in non-squamous histology, pemetrexed has shown to produce better outcomes than gemcitabine<sup>4</sup>.

The discovery of driver molecular alterations, such as *EGFR* mutations<sup>5, 6</sup> and most recently ALK-fusion<sup>7</sup> predominantly in never-smokers<sup>8</sup>, has unraveled a new horizon in the treatment of lung adenocarcinomas. The concept of “oncogene addiction”<sup>9</sup> has created the basis for the successful use of targeted therapy of genetic alterations (i.e., erlotinib and crizotinib) changing therefore the therapeutic approach to this particular subtype of NSCLC<sup>10</sup>, as cancers harboring these genetic alterations are dependent on the expression of these single mutant oncogenes for survival. In the last decade, extensive literature has been published on genetic alterations that arise in lung adenocarcinoma from never smokers, however little is known about potential targets of smoking-related lung adenocarcinoma. Known driving mutations found in lung adenocarcinomas from smokers are *KRAS* and *BRAF*, however more efforts need to be implied to discover novel targets in this setting<sup>11</sup>.

The major role of chemokines is to act as a chemoattractant to guide the migration of cells. Cells that are attracted by chemokines follow a signal of increasing chemokine

concentration towards the source of the chemokine. Chemokines are functionally divided in two groups: homeostatic which are constitutively produced in certain tissues and are responsible for basal leukocyte migration (CCL14, CCL19, CCL20, CCL21, CCL25, CCL27 and CXCL12, CXCL13) and inflammatory which are produced under pathological conditions (i.e., on pro-inflammatory stimuli such as IL-1, TNF-alpha, viruses) and actively participate in the inflammatory response attracting immune cells to the site of inflammation (i.e., CXCL8, CCL2, CCL3, CCL4, CCL5, CCL11, CXCL10)<sup>12</sup>. Members of the chemokine family are divided into four groups depending on the spacing of their first two cysteine residues: CC chemokines with 2 adjacent cysteines, CXC chemokines in which the two N-terminal cysteines are separated by one amino acid, C chemokines with only two cysteines and CXC3C chemokines with 3 amino acids between the two cysteines. CXC chemokines have multiple roles in the tumor microenvironment<sup>13; 14; 15</sup> and they are expressed on multiple cells including neutrophils, monocytes, eosinophils, mast cells, basophils, lymphocytes, epithelial cells, and endothelial cells<sup>16; 17</sup>. One of the most important functions is to mediate communication between different cells in the tumor microenvironment and immune system<sup>16</sup>. CXC chemokines containing the sequence Glu-Leu-Arg (ELR motif) as compared with members that lack these 3 amino acids are potent inducers of angiogenic activity as these 3 amino acids appear to be important in ligand/receptor interactions on neutrophils<sup>18</sup>.

Two G-protein-coupled receptors, CXCR1 and CXCR2, and the Duffy antigen receptor, are the three known receptors for these chemokines. Endothelial cells and neutrophils express CXCR2 and migrate toward sites of CXCR2 ligand production such as inflammatory foci or nascent tumors, thereby promoting angiogenesis and inflammation in tumors that express ELR-positive CXC chemokines<sup>19; 20; 21; 22</sup>. CXCR2 binds CXCL8 (IL-8), CXCL1, 2, and 3 (GRO $\alpha$ ,  $\beta$ , and  $\gamma$ ), CXCL5 (ENA-78), CXCL6 (GCP2), and

CXCL7 (NAP2), whereas CXCR1 binds only to GCP2, NAP2, and IL-8. Chemokine receptors associate with G-proteins to transmit cell signals following ligand binding. Activation of G proteins, by chemokine receptors, causes the subsequent activation of the phospholipase C (PLC) with subsequent activation of the mitogen-activated protein (MAP) Kinase pathway activation with induction of chemotaxis, degranulation, release of superoxide anions and changes in the avidity of integrins within the cell harboring the chemokine receptor<sup>23</sup>.

In particular CXCR2 couples to the pertussis toxin-sensitive G<sub>i</sub> proteins to stimulate PLC-β which ultimately results in hydrolysis of the lipid phosphatidylinositol 4,5-bisphosphate, generating diacylglycerol, which activates PKC isoforms, and inositol 1,3,4-triphosphate, which releases calcium from intracellular stores. In addition, recently CXCR2 has been found to contain specific modular protein interaction domains called PDZ domains that may be responsible to nucleate the formation of compartmentalized multiprotein complexes that are critical for efficient and specific cellular signaling with scaffold proteins<sup>24; 25</sup>.

Expression of the ELR+ CXC chemokines in human NSCLC samples correlates with worse survival<sup>26; 27</sup>. Wislez M. et al. showed that CXCR2 ligands are abundant in alveolar epithelial cells of lung tumors arising in mice expressing *KRAS*<sup>G12D</sup> alone and in combination with a *Tp53* mutation (*p53*<sup>R172H</sup>) or *Pten* deletion<sup>28; 29; 30; 31; 32; 33</sup>. CXCR2 neutralization decreased tumor angiogenesis and neutrophilic inflammation and blocked the expansion of early alveolar neoplastic lesions in *KRAS*<sup>LA1</sup> mice without having direct effects on tumor cells, implicating the tumor microenvironment in the anti-tumor effect of CXCR2 inhibition<sup>33</sup>.

However, there is controversial data in the literature about CXCR2 expression in tumor cells and its role on tumor growth and angiogenesis<sup>20; 34; 35; 36; 37</sup>. Preclinical models have shown that CXCR2 expression can impact cell proliferation, migration, invasion and stress-induced apoptosis evasion<sup>14; 38; 39; 40; 41</sup>. There are missing data, however, about if these effects are mediated by a direct effect of CXCR2 expression on cancer cells or by an anti-angiogenesis effect<sup>20; 39; 42; 43</sup>. Pharmaceutical inhibition of CXCR2 is currently undergoing clinical development in chronic obstructive pulmonary disease (COPD) to counter-act the damaging effects of cigarette smoking that produces inflammation with increase in alveolar destruction by neutrophils, goblet cell hyperplasia and pro-angiogenic effects<sup>17; 44</sup>. These compounds therefore may be eventually available to be used to target the CXCR2 expression on cancer cells in the future.

Among the CXCR2 inhibitors, SB225002 (*N*-(2-hydroxy-4-nitrophenyl)-*N*-(2-bromophenyl)urea) was the first reported potent and selective non-peptide inhibitor of CXCR2. It is an antagonist of IL-8 binding to CXCR2 with an  $IC_{50} = 22$  nM. SB 225002 showed >150-fold selectivity over CXCR1 and four other chemokine receptors tested. This compound inhibited the binding of both CXCL8 and CXCL1 on recombinant and native CXCR2 and also blocked CXCL8 and CXCL1-induced chemotaxis and margination of human and rabbit neutrophils without having any affinity or activity on CXCR1<sup>45</sup>.

To clarify the effect of CXCR2 inhibition in NSCLC, I hypothesized that CXCR2 ligands promote tumor invasion and metastasis in NSCLC. I proposed to test this hypothesis by investigating the CXCR2 role in a *KRAS/p53*-mutant lung adenocarcinoma murine model *in vitro* and *in vivo*<sup>46; 47; 48</sup>. To understand the potential translational significance of my work in human NSCLC, CXCR2 tumoral expression was assessed in tissue microarrays of human NSCLC from stage I-II patients in correlation with patients

clinicopathological characteristics and a systematic analysis of gene expression profiles of *CXCR2* and its ligands (subsequently called the *CXCR2* axis) was conducted in human NSCLC cell lines and lung adenocarcinomas.



## **MATERIALS AND METHODS**

This thesis is based upon the following article: *Massarelli E. and Saintigny P, Lin S, Ahn Y-H, Chen Y, Goswami S, Erez B, O'Reilly MS, Liu D, Lee JJ, Zhang L, Ping Y, Berhens C, Solis Soto LM, Heymach JV, Kim ES, Herbst RS, Lippman SM, Wistuba II, Hong WK, Kurie JM. Cancer Research. 2013 Jan 15; 73(2):571-82. DOI: 10.1158/0008-5472*. This material is reprinted by permission from the American Association for Cancer Research.

### ***Human lung tissues and tissue microarray***

A detailed description of the tissue microarray (TMA) construction is provided elsewhere<sup>49</sup>. In summary, after histological examination of NSCLC specimens, the NSCLC TMAs were constructed by obtaining three 1-mm in diameter cores from each tumor at three different sites (periphery, intermediate and central tumor sites).

### ***Immunohistochemical analysis***

Mouse monoclonal anti-human CXCR2 antibody (R&D Systems, Minneapolis, MN) was used at a dilution of 1:200, according to the manufacturer's instruction. CXCR2 staining was examined using light microscopy by a lung cancer pathologist (Dr. Yuan Ping). An independent observer (Dr. Ignacio I. Wistuba) reviewed one third of the cores chosen randomly. In case of discordance (~10%), both pathologists reviewed the slides jointly in a multiheaded microscope and reached consensus. Both pathologists were blinded with respect to the patients' outcome. Only cytoplasmic CXCR2 expression was quantified using a four-value intensity score (0, 1+, 2+, and 3+) and extent of reactivity (0-100%). Final score was then obtained by multiplying the intensity and reactivity extension values (range, 0-300).

### ***Animal husbandry***

All animal experiments were reviewed and approved by the Institutional Animal Care and Use Committee at MD Anderson Cancer Center. For syngeneic tumor experiments, 10- to 16- week-old 129/Sv mice were injected with the indicated numbers of tumor cells into the left lung and euthanized at the first signs of morbidity.

### ***Establishment of murine lung adenocarcinoma cell lines***

The methods used to establish lung adenocarcinoma cell lines in culture from murine tumors have been described previously<sup>46</sup>. Cell lines were named according to the mouse number and site of derivation (e.g., 344SQ for mouse 344, subcutaneous metastasis). These cells have alveolar type II cell properties and variable propensities to undergo the epithelial-to-mesenchymal transition and metastasize following injection into syngeneic mice<sup>46; 48</sup>.

### ***RNA extraction and quantitative reverse-transcription PCR***

RNAs were extracted using TRIzol (Invitrogen, Carlsbad, CA). mRNA was reverse transcribed using the SuperScript First-Strand Synthesis System (Invitrogen). For quantitative PCR reactions, 1:10 dilutions of cDNA products were amplified by using SYBR Green PCR Master Mix (Applied Biosystems,

Carlsbad, CA) and analyzed by using ABI Prism 7500 Fast System (Applied Biosystems). mRNA expression values were normalized on the basis of L32 mRNA.

#### **Generation of shRNA transfectants**

The shRNA retroviral *CXCR2* constructs were purchased (OriGene, Rockville, MD). The sequences of the *CXCR2* and scrambled shRNA were as follow: CAAGGTGGATAAGTTCAACATTGAAGATT (*CXCR2* clone 1), GTCTGCTATGAGGATGTAGGTAACAATAC (*CXCR2* clone 3), and GCACTACCAGAGCTAACTCAGATCGTACT (scrambled shRNA). Purified plasmids (1 µg of each) were transfected into 344SQ cells by using LipofectAmine and PLUS (Invitrogen). After 48 hours, transfectants were replated in RPMI 1640 medium containing 10% FBS and 15 µg/ml puromycin for selection and passed serially for 4 weeks to generate stable transfectants.

#### **Cell invasion assay**

As described previously<sup>46</sup>, cells (cancer-associated fibroblasts) were seeded first in the lower chambers (105 cells), and tumor cells (344SQ) were then seeded in the upper chambers ( $5 \times 10^4$ ) of 24-well Transwell invasion plates (BD Biosciences, Bedford, MA) in serum free medium containing mitomycin C to block proliferation. Cells in the upper chambers were allowed to invade for 14 to 16 hours. Cells on the inserts were fixed with 90% ethanol, stained with 0.1% crystal violet blue, and washed with ddH<sub>2</sub>O. Noninvaded cells on the upper side of the inserts were wiped off with a cotton swab. Invaded cells were counted in five microscopic fields at 4x magnification, and the counts were averaged. A small molecule antagonist of *CXCR2* (SB225002) (Calbiochem) was used to inhibit *CXCR2* invasive properties of 344P cells in Boyden chamber assays and included 344SQ cells as positive controls<sup>45; 50</sup>.

#### **Gene expression analysis**

Publicly available gene expression profiles and clinical annotations of 442 lung adenocarcinomas were downloaded from the NCI Director's Challenge Consortium for the Molecular Classification of adenocarcinoma (DCC)<sup>51</sup>. CEL files of 52 NSCLC cell lines (GSE4824)<sup>52; 53</sup>, 130 lung squamous cell carcinomas with clinical annotations (GSE4573)<sup>54</sup>, and 7 NSCLC cell lines and 3 human bronchial epithelial cell lines (HBEC) before and after treatment with 5-aza-2'-deoxycytidine (decitabine) (GSE5816)<sup>55</sup> were downloaded from Gene Expression Omnibus (GEO). The gene expression analysis was generated by using Array Studio software (Omicsoft Corporation, Research Triangle Park, NC). Raw microarray data were processed using quantile normalization and robust multi-array average algorithm. Probesets corresponding to *CXCR2* axis were identified using the NetAffx Analysis Center from Affymetrix website. They were used to compute an unsupervised hierarchical clustering of the cell lines and of the lung adenocarcinomas using the Pearson's correlation coefficient and Ward's linkage method. To summarize the effect of *CXCR2* axis, a principal component analysis was computed with the first two components. In the DCC, the first principal component (PC1) was used for correlative studies with tumor differentiation, smoking status, and overall survival. In the cell lines, PC1 was correlated with the whole genome. Gene Set Enrichment Analysis (GSEA) using the "pre-ranked" tool was done using either the genes ranked according to their correlation with PC1, or to fold-change between groups defined by the unsupervised hierarchical clustering. Probesets with an absolute Pearson correlation or a fold-change  $\geq 0.5$  were included in network analyses performed using Ingenuity Pathway Analysis

(IPA) (Ingenuity® Systems, Redwood City, CA). Details of the GSEA and IPA are provided in Supplementary Material and Methods.

#### **CXCL5 promoter methylation study**

*CXCL1*, *CXCL2*, *CXCL3*, *CXCL5* and *CXCL6* promoter methylation status was obtained from high-throughput promoter methylation profiles of 42 NSCLC cell lines overlapping with the panel of 52 NSCLC cell lines analyzed for gene expression. *CXCL7* and *CXCL8* results did not pass the quality control and were not included in the analysis. DNA methylation status of a set of 27,579 CpG sites around promoters of 14,475 consensus coding sequences was interrogated using the Illumina HumanMethylation27 Beadchip (Illumina, Inc., San Diego, CA). Genomic DNA (1 µg) was bisulfite-converted using the EZ DNA Methylation kit (Zymo Research Corp, Orange CA). Whole-genome amplification, fragmentation, hybridization, washing, counterstaining, and scanning were performed according to the manufacturer's instructions. The scanner data and image output files were managed with the Illumina BeadStudio software Methylation module v.3.2. The normalized data, presented as beta values, represent the degree of methylation at each CpG site, 0 being unmethylated and 1 being methylated.

#### **Gene Set Enrichment Analysis**

GSEA is a robust computational method that determines whether an *a priori* defined set of genes shows statistically significant, concordant correlation with the *CXCR2/CXCR2* ligands biological axis. GSEA aims to interpret large-scale expression data by identifying pathways and processes<sup>56</sup>. The main advantage of this method is its flexibility in creating molecular signature databases of gene sets, including ones based on biologic pathways, or expression profiles in previously generated microarray data sets. The input data for the GSEA<sup>56</sup> were the following: (1) a complete table of genes ranked according to their Pearson correlation with PC1, (2) a mapping file for identifying probesets in HG-U133A and B platforms, and (3) a catalog of functional gene sets from Molecular Signature Database (MSigDB, version 3.0, 30-September-2010 release, [www.broad.mit.edu/gsea/msigdb/msigdb\\_index.html](http://www.broad.mit.edu/gsea/msigdb/msigdb_index.html)). A total of 2,480 curated gene sets (canonical pathway gene sets, chemical and genetic perturbations gene sets, BioCarta gene sets, GenMAPP gene sets, and KEGG gene sets) were included in the analysis. Default parameters were used. Probesets (44,754 unique features in cell lines, 22,283 unique features in lung adenocarcinomas) were collapsed into gene symbols (18,770 unique genes in cell lines, 13,321 unique genes in lung adenocarcinomas). Inclusion gene set size was set between 15 and 500, and the phenotype was permuted 1,000 times. Gene sets that met the false discovery rate 0.25 criterion were considered.

#### **Ingenuity Pathway Analysis**

Probesets with an absolute Pearson correlation or a fold-change equal to or greater than 0.5 were included in network analyses performed using Ingenuity Pathway Analysis (Ingenuity® Systems, [www.ingenuity.com](http://www.ingenuity.com)). Network Generation: a data set containing gene identifiers and corresponding expression values was uploaded into the application. Each gene identifier was mapped to its corresponding gene object in the Ingenuity Pathways Knowledge Base. These genes, called focus genes, were overlaid onto a global molecular network developed from information contained in the Ingenuity Pathways Knowledge Base. Networks of these focus genes were then algorithmically generated based on their connectivity. Network/My Pathways Graphical Representation: a Network/My Pathways is a graphical representation of the molecular relationships between genes/gene products. Genes or gene products are

represented as nodes, and the biological relationship between two nodes is represented as an edge (line).

All edges are supported by at least one reference from the literature, from a textbook, or from canonical information stored in the Ingenuity Pathways Knowledge Base. Human, mouse, and rat orthologs of a gene are stored as separate objects in the Ingenuity Pathways Knowledge Base, but are represented as a single node in the network. The intensity of the node color indicates the degree of positive (red) or negative (green) correlation. Nodes are displayed using various shapes that represent the functional class of the gene product. Edges are displayed with various labels that describe the nature of the relationship between the nodes.

### ***Statistical analysis***

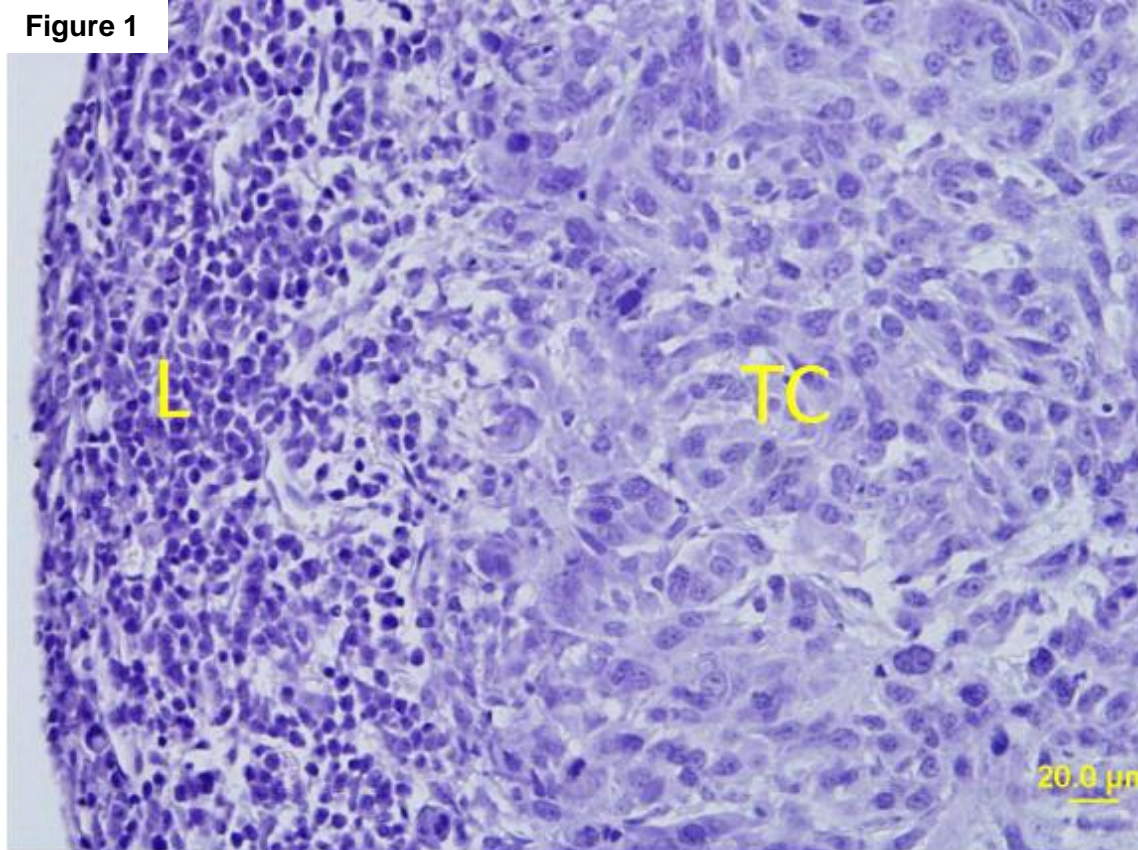
Wilcoxon rank sum test or Kruskal-Wallis test was used to test the differences of CXCR2 expression between/among categorical variable levels. Martingale residuals were performed from a Cox model that included only baseline hazard function but no covariate. By applying a nonparametric smoother, the plots allow one to examine visually the nature of the relationship between the residuals and CXCR2 H-scores and to define a reasonable cutoff point to dichotomize the population. The Kaplan-Meier method was used to construct overall and recurrence-free survival curves, and the log-rank test was used to test the difference by covariate levels. Univariate and multivariate Cox models were fitted to estimate the effect of prognostic factors, including patient age, sex, tumor histology, stage, and marker on time to event endpoint. For cell line experiments, comparisons between two groups were performed using the Wilcoxon rank sum test unless otherwise indicated. One-way ANOVA was performed to compare multiple experimental groups. All statistical tests were two-sided, and *P*-values of 0.05 or less were considered to be statistically significant.

## **RESULTS**

### ***Creation of an orthotopic syngeneic lung adenocarcinoma metastasis model***

We recently described the creation of a panel of cell lines from *Kras*<sup>LA1/+</sup>*p53*<sup>R172H</sup> $\Delta$ *G*<sup>+</sup> mice, which develop aggressive and metastatic lung adenocarcinoma<sup>48</sup>. One of these cell lines, 344SQ, is highly metastatic when injected subcutaneously into syngeneic mice<sup>46</sup>. In order to refine our lung adenocarcinoma metastasis model, we used 344SQ to create a novel orthotopic syngeneic model. As previously described<sup>57</sup>,  $2 \times 10^4$  344SQ cells were injected into the left lung of syngeneic mice. The mice were euthanized 21 days after injection and, at necropsy, had developed metastases to hilar and mediastinal lymph nodes (Fig. 1), chest wall, and contralateral lung as well as extrathoracic distant metastases in the paraaortic lymph nodes, liver, adrenal glands, kidneys, spleen and diaphragm.

**Figure 1. Mediastinal lymph node metastasis from an orthotopic lung tumor.** Hematoxylin and eosin-stained tissue section of a mediastinal lymph node from a mouse injected intrathoracically (left lung) with 344SQ cells ( $2 \times 10^4$ ), killed after 21 days, and subjected to necropsy (L: lymphocytes; TC: tumor cells)



***CXCR2 knockdown decreased tumor cell invasion in vitro***

To investigate the role of CXCR2 expression by tumor cells, we created CXCR2 shRNA clones from parental 344SQ lung adenocarcinoma cell lines isolated from *KrasLA1/+p53R172HΔG/+* mice. CXCR2 shRNA clones exhibited significantly lower expression of CXCR2 mRNA than scrambled controls (Fig. 2A). To test the invasion potential of the shRNA clones, we used cocultures with cancer-associated fibroblasts, which produce high levels of CXCR2 ligands, as previously described<sup>58</sup>. To block tumor cell proliferation, we added mitomycin C to the serumfree medium in which the tumor cells were cultured (344SQ). CXCR2 shRNA clones showed a significantly lower invasion potential than scrambled controls (Fig. 2B).

***CXCR2 pharmacological inhibition decreased tumor cell invasion in vitro***

To confirm our findings in the 344SQ cells, we carried out experiments by using 344P, a second highly invasive and metastatic lung adenocarcinoma cell line derived from *KrasLA1/+p53R172HΔG/+* mice. To inhibit CXCR2 using a different approach, we used a small molecule antagonist of CXCR2, SB225002, that has demonstrated selectivity and potency *in vitro* and *in vivo*<sup>45; 50</sup>. We examined the effect of SB225002 on 344P cell invasive properties in Boyden chamber assay and included 344SQ cells as a positive control. Treatment with SB225002

inhibited tumor cell invasive properties with an IC<sub>50</sub> of 3-4 μmol/L for both 344P cells and 344SQ cells (Fig. 2C-D).

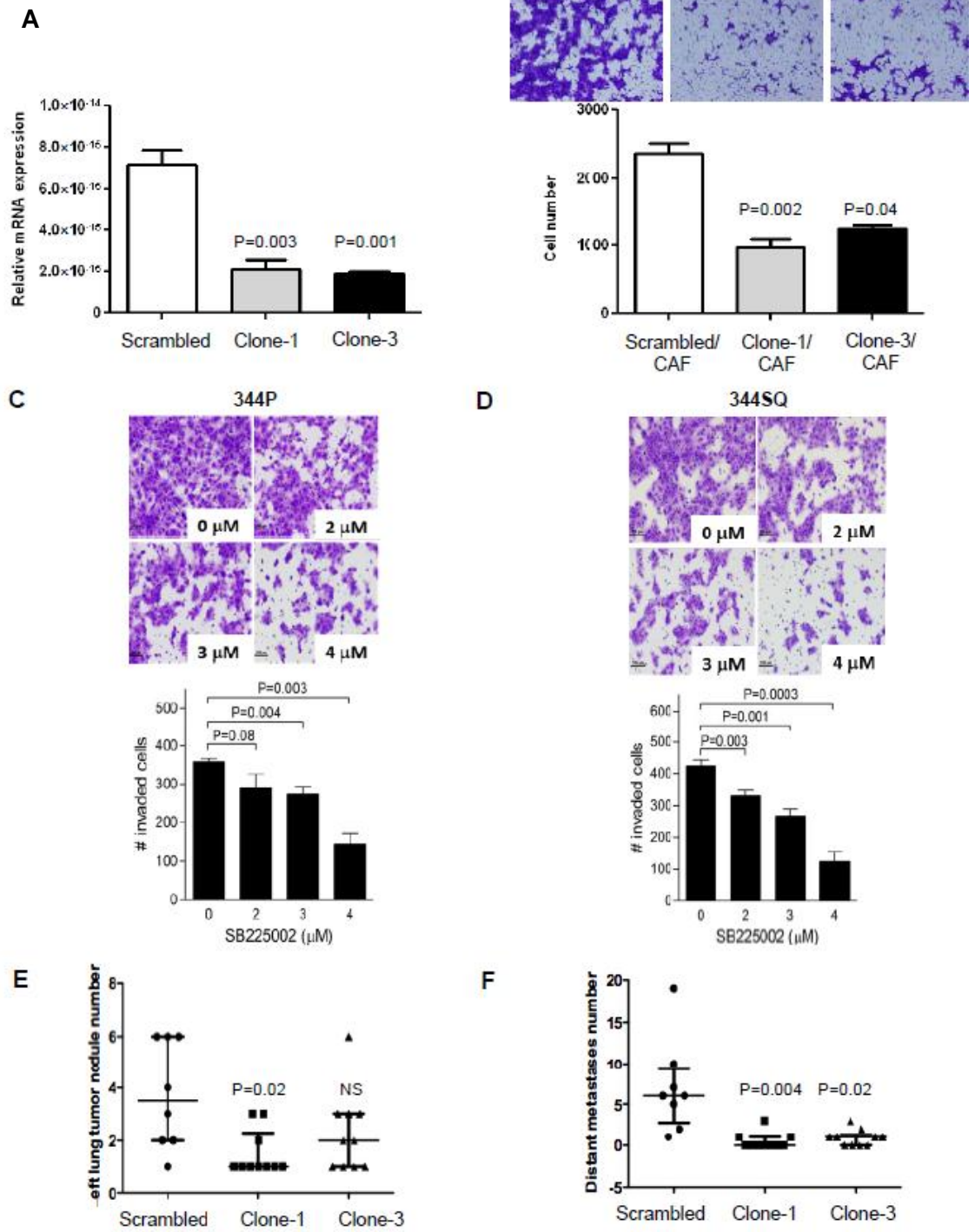
***CXCR2 knockdown in tumor cells decreased 344SQ metastatic potential***

We used the orthotopic murine model already described to test whether the metastatic potential of 344SQ would be affected by *CXCR2* knockdown. Two shRNA clones (clone-1 and clone-3) and scrambled controls were compared by injecting 2x10<sup>4</sup> cells into the left lung of mice (N=10 in each group, for a total of 30 mice). Mice were euthanized at 21 days after injection because two of the 10 mice in the scrambled control group demonstrated poor physical conditions due to tumor burden. At necropsy, mice bearing *CXCR2*-shRNA lung adenocarcinoma had significantly fewer lung tumor nodules in the lung of primary injection (Fig. 2E) and fewer distant metastases (Fig. 2F) than scrambled controls. Sites of distant metastases included liver, adrenal glands, ipsilateral and contralateral lung, diaphragm, spleen and paraortic lymph nodes.

**Figure 2. Effect of *CXCR2* downregulation and inhibition.** *In vitro* (A-B) properties of shRNA clones (clone-1 and -3) compared to scrambled control: (A) mRNA expression by reverse transcription PCR relative to standard, (B) invasion assay using co-cultures with cancer associated fibroblasts (CAF) and mitomycin C to block tumor cell proliferation. *In vitro* *CXCR2* inhibition with *CXCR2*-antagonist (C, D): invasion assay using co-cultures of 344P (C) and 344SQ (D) cell lines treated with increasing concentrations of SB225002. *In vivo* properties of shRNA clones (clone-1 and -3) compared to scrambled control (E, F): number of left lung tumor nodules, (E) number of distant metastases (F). Median and inter-quartile range are shown in the dot plots (E, F). Wilcoxon rank sum test (A, B, E, and F) between scrambled control and shRNA single clones (clone-1 and clone-3) or between different concentrations of SB225002 and the control (C, D).



**Figure 2**



***CXCR2 protein expression in human NSCLC tumor cells is associated with adverse outcome and tobacco smoking***

To investigate the role of CXCR2 in human tumor cells, we stained a tissue microarray that included 370 resected NSCLC. For the purpose of this study, we considered only 262 patients with stage I and II disease who did not receive preoperative chemotherapy. Clinical and pathological characteristics of the patient population are described in Table 1. Median age was 67.4 years (range: 32.2-90.0). Adenocarcinoma was the most frequent histological subtype (N=173, 66%). With a median follow-up of 5.3 years, 133 patients had developed recurrence (50.8%) and 101 had died (38.5%).



**Table 1.** Clinical and pathological characteristics of patients included in the tissue microarray (N=262).

Covariate	N (%)
<b>Sex</b>	
F	134(51.1%)
M	128(48.9%)
<b>Race</b>	
Other	22(8.4%)
White	240(91.6%)
<b>Smoking status</b>	
Current	105(40.1%)
Former	127(48.5%)
Never	30(11.5%)
<b>Pathological stage</b>	
I	201(76.7%)
II	61(23.3%)
<b>Histology</b>	
Adenocarcinoma	173(66%)
Squamous cell carcinoma	89(34%)
<b>Degree of differentiation</b>	
Poor	74(28.2%)
Moderate	155(59.2%)
Well	33(12.6%)
<b>Degree of inflammation</b>	
Mild	106(41.1%)
Moderate	106(41.1%)
Severe	46(17.8%)
Unknown	4
<b>Adjuvant therapy</b>	
No	180(71.4%)
Yes	72(28.6%)
Unknown	10

CXCR2 was expressed mainly in the cytoplasm (mean  $31.07 \pm 30.78$ , median 20, range 0-130). Distribution of cytoplasmic CXCR2 protein expression in the whole population is shown in Fig. 3.

**Figure 3. Distribution of cytoplasmic CXCR2 protein expression.** Distribution of cytoplasmic CXCR2 protein expression in 262 non small cell lung cancer cell lines by squamous cell carcinoma (SCC) and adenocarcinoma (Adeno) histology.

**Figure 3**

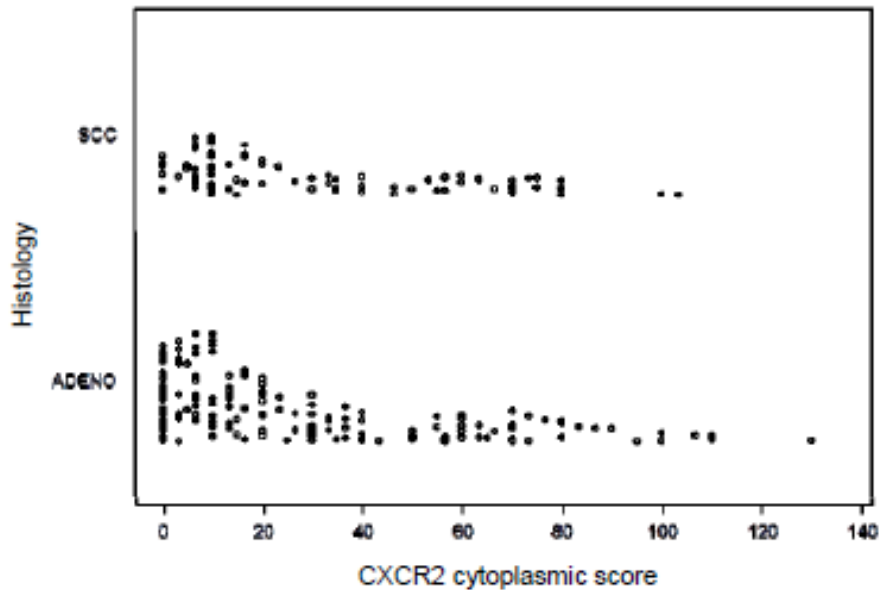
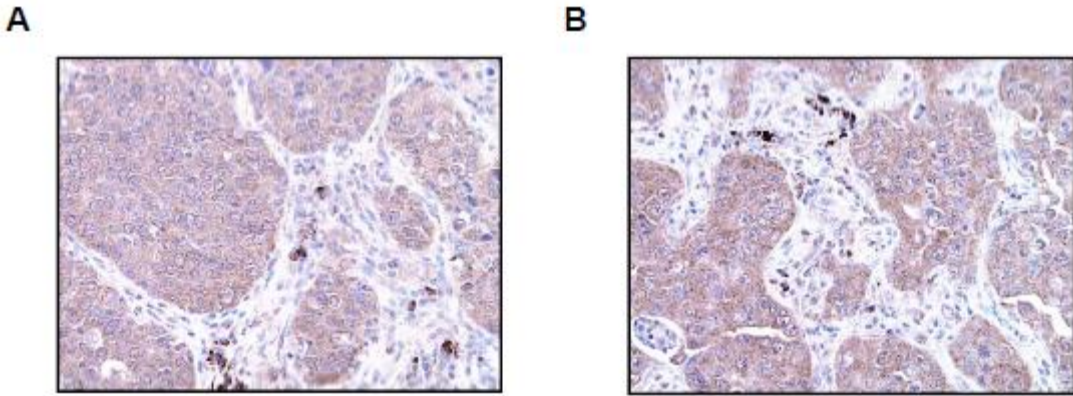


Figure 4 shows one adenocarcinoma and one squamous cell carcinoma expressing CXCR2 with an intensity of 1 in 100% of tumor cells, and an H-score of 100. CXCR2 expression was low in the nucleus (mean  $16.15 \pm 24.88$ , median 3.33, range 0-120). Cytoplasmic and nuclear CXCR2 expression levels were not correlated ( $\rho = -0.02$ ,  $P = 0.76$ ). No association was observed between cytoplasmic CXCR2 and patient sex, race, tumor histology, stage or degree of inflammation. Cytoplasmic CXCR2 expression was higher in current smokers ( $32.57 \pm 28.28$ ) and former smokers ( $31.19 \pm 33.15$ ) than in never smokers ( $25.28 \pm 29.00$ ), although it did not reach statistical significance. Similarly, poorly differentiated tumors had higher cytoplasmic CXCR2 levels ( $39.84 \pm 32.20$ ) than moderately ( $29.99 \pm 30.18$ ) or well-differentiated ( $16.46 \pm 23.98$ ) tumors ( $P < 0.0001$ ).

**Figure 4. Expression of CXCR2 in tumor cells and tissues.** Immunohistochemical expression of CXCR2 in two NSCLC tissue specimens, (A) squamous cell carcinoma and (B) adenocarcinoma.

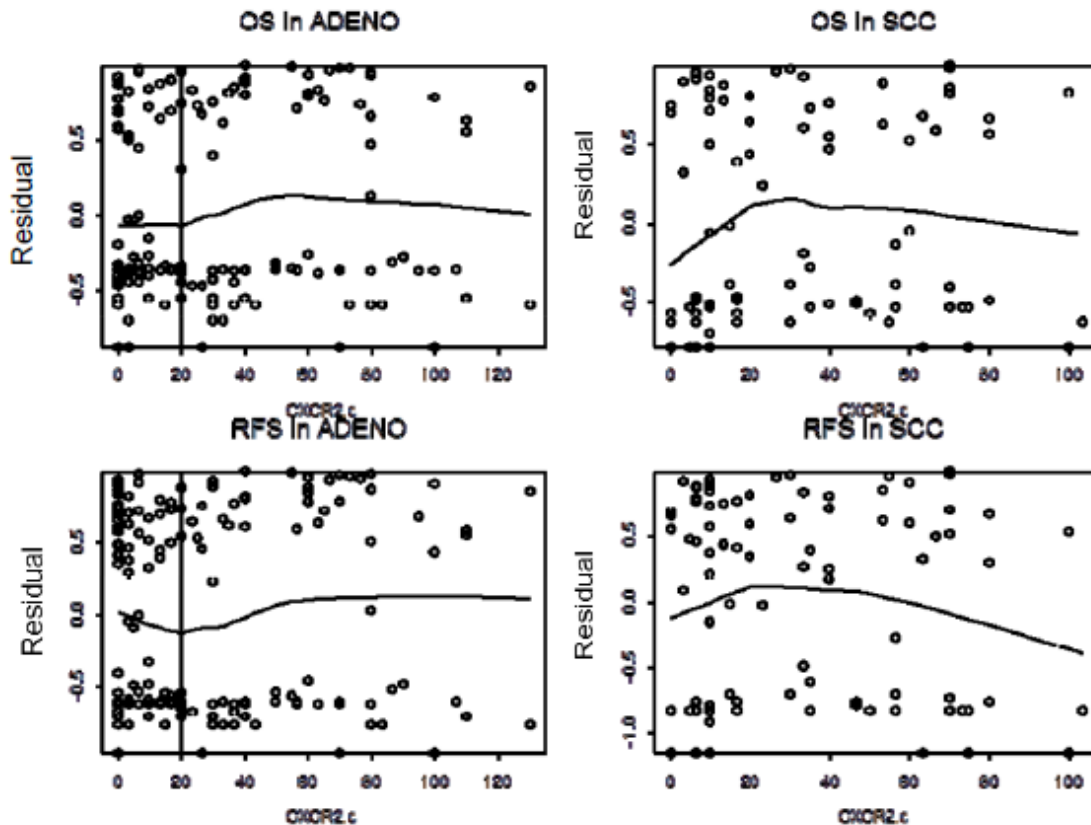
**Figure 4**



The Martingale residual plots showed that median CXCR2 H-score was a reasonable cutoff point (Fig. 5).

**Figure 5. Median CXCR-2 immunohistochemistry score.** Martingale residuals analysis from a Cox model that includes only baseline hazard function but no covariate, are represented on the vertical axis and CXCR2 H-scores (CXCR2c) are represented on the horizontal axis. The median H-score for CXCR2 expression is shown by a vertical bar.

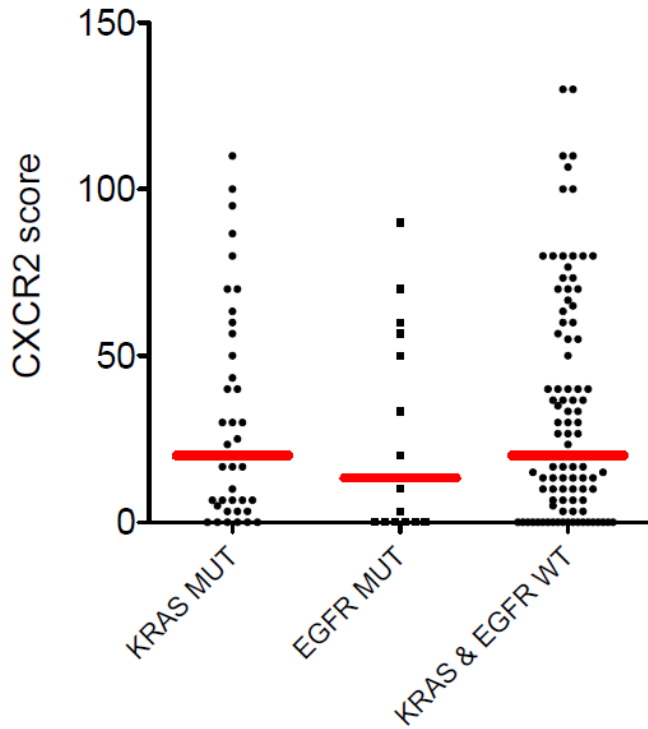
Figure 5



When cytoplasmic CXCR2 level was dichotomized using the median expression of 20, 141 (53.8%) tumors expressed low CXCR2 levels ( $\leq 20$ ) and 121 (46.2%) tumors expressed high CXCR2 levels ( $> 20$ ). *EGFR* and *KRAS* mutational status was available for 157 of the lung adenocarcinomas; Figure 6 shows that cytoplasmic CXCR2 protein expression was lower, although not reaching statistical significance, in *EGFR*-mutant lung adenocarcinomas (N=17, mean  $24.71 \pm 29.49$ , median 13.33, range 0-90), which are known to be more frequent among never smokers, than in *KRAS*-mutant (N=41, mean  $31.02 \pm 31.65$ , median 20, range 0-110) or wild-type *EGFR* and wild-type *KRAS* lung adenocarcinomas (N=99, mean  $33.05 \pm 33.61$ , median 20, range 0-130), which are more frequent among smokers.

**Figure 6. CXCR2 expression according to EGFR and KRAS mutation status.**  
CXCR2 expression in tumor cells according to *EGFR* and *KRAS* mutation status. *EGFR* and *KRAS* mutation status was available for 157 lung adenocarcinomas analyzed for cytoplasmic CXCR2 protein expression.

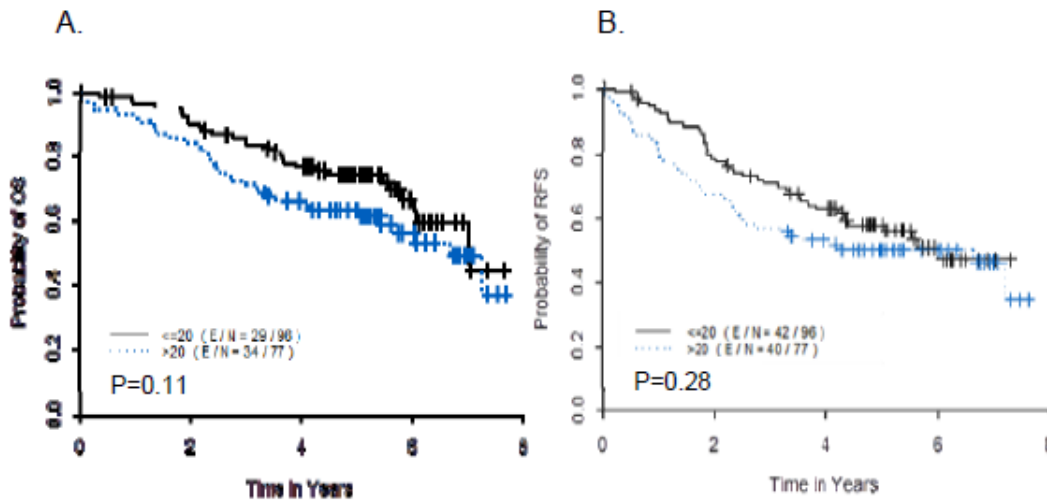
**Figure 6**



Using Kaplan-Meier curves, high CXCR2 expression was associated with poor overall survival and recurrence-free survival in patients with lung adenocarcinoma, although not reaching statistical significance (Fig. 7A-B).

**Figure 7. Overall survival and recurrence-free survival as a function of cytoplasmic CXCR2 expression in lung adenocarcinoma.** Kaplan-Meier curves for (A) overall survival and (B) recurrence-free survival as a function of cytoplasmic CXCR2 expression in 173 patients who underwent resection for lung adenocarcinoma.

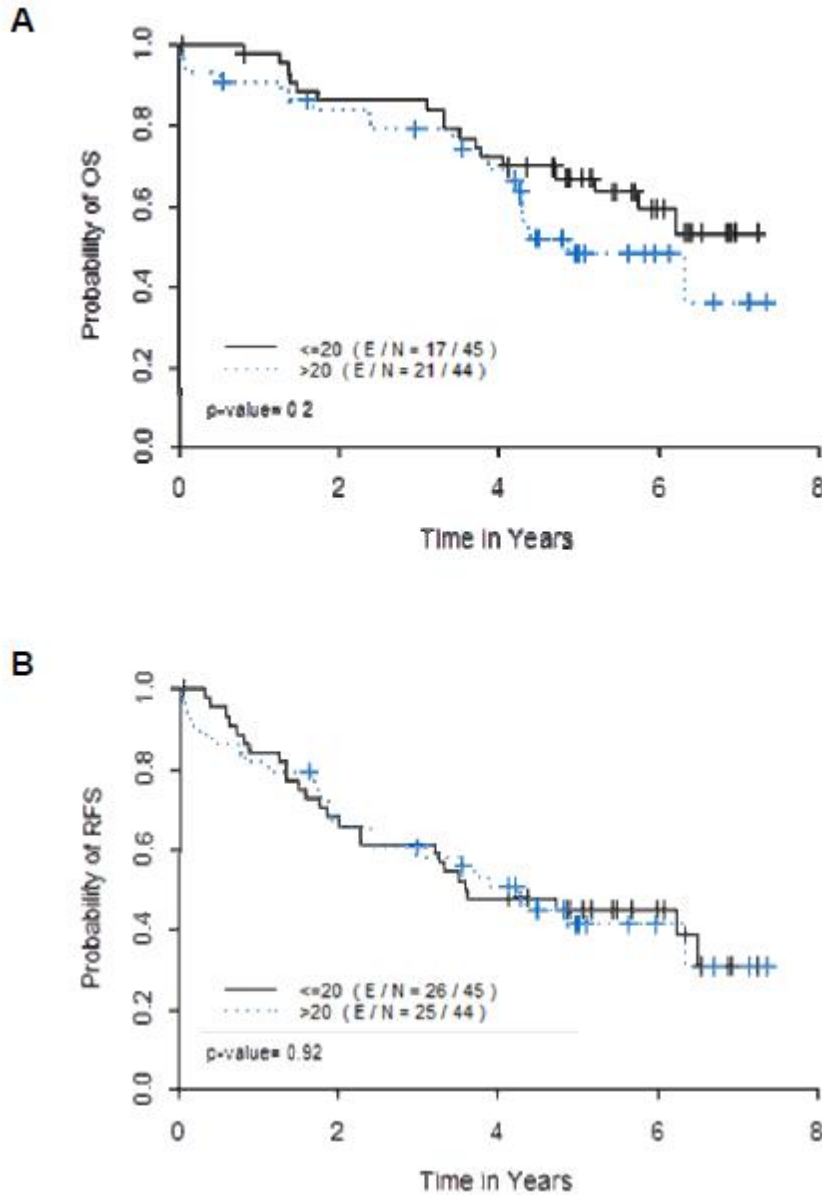
**Figure 7**



No such association was observed in patients with squamous cell carcinoma (Fig. 8A-B).

**Figure 8. Overall survival and recurrence-free survival as a function of cytoplasmic CXCR2 expression in lung adenocarcinoma.** Kaplan-Meier curves for (A) overall survival and (B) recurrence-free survival as a function of cytoplasmic CXCR2 protein expression in 89 patients who underwent resection for lung squamous cell carcinoma.

**Figure 8**



Univariate Cox proportional hazards model assessed the effect of covariates on survival. High CXCR2 expression was associated with worse overall survival in both subtypes [hazard ratio (HR) =1.488 95% confidence interval (95%CI): 0.905-2.448; HR=1.520 95%CI: 0.798-2.894] (Table 2A and 3A), although not reaching statistical significance. For recurrence-free survival, a similar trend was observed in adenocarcinoma (HR=1.284 95%CI: 0.830-1.985), but not in

squamous cell carcinoma (HR=1.028 95%CI 0.593-1.782) (Table 2B and Table 3B).

**Table 2.** Univariate Cox model assessing the effect of covariates on overall survival (A) and recurrence-free survival (B) (M: male; F: female; HR: hazard ratio; 95CI: 95% confidence interval), in adenocarcinoma patients (N=173).

**A**

Covariate	HR	95%CI		P
Age	1.015	0.989	1.041	0.2624
Sex (M vs. F)	2.088	1.264	3.451	0.004
Race (White vs. Other)	0.828	0.356	1.923	0.6603
Smoking history				
Former vs. Never	1.110	0.525	2.346	0.7852
Current vs. Never	1.131	0.526	2.432	0.7531
Pathological stage (II vs. I)	2.067	1.192	3.583	0.01
Degree of differentiation				
Poor vs. Well	1.324	0.630	2.783	0.4595
Moderate vs. Well	2.144	0.991	4.641	0.0528
Degree of inflammation				
Moderate vs. Mild	0.971	0.552	1.705	0.9173
Severe vs. Mild	0.986	0.504	1.928	0.9665
Adjuvant treatment (Yes vs. No)	0.805	0.433	1.496	0.4927
CXCR2 (>20 vs. ≤20)	1.488	0.905	2.448	0.1172

**B**

Covariate	HR	95% CI		P
Age	1.012	0.990	1.035	0.2891
Sex (M vs. F)	1.542	0.999	2.379	0.0504
Race (White vs. Other)	1.129	0.491	2.596	0.7747
Smoking history				
Former vs. Never	1.134	0.596	2.159	0.7015
Current vs. Never	0.996	0.508	1.956	0.9918
Pathological stage (II vs I)	2.471	1.520	4.016	0.0003
Degree of differentiation				
Poor vs. Well	1.250	0.674	2.318	0.4783
Moderate vs. Well	1.375	0.699	2.701	0.3560
Degree of inflammation				
Moderate vs. Mild	0.675	0.411	1.107	0.1191
Severe vs. Mild	0.712	0.389	1.304	0.2710
Adjuvant treatment (Yes vs. No)	1.175	0.715	1.929	0.5247
CXCR2 (>20 vs. ≤20)	1.284	0.830	1.985	0.2610



**Table 3.** Univariate Cox model assessing the effect of covariates on overall survival (A) and recurrence-free survival (B) (M: male; F: female; HR: hazard ration; 95CI: 95% confidence interval), in squamous cell carcinoma patients (N=89).

**A**

Covariate	HR	95%CI	P	
Age	1.016	0.981	1.052	0.3791
Sex (M vs. F)	0.975	0.514	1.849	0.9379
Race (White vs. Other)	0.163	0.060	0.440	0.0003
Smoking history				
Former vs. Never	0.258	0.034	1.971	0.1915
Current vs. Never	0.356	0.047	2.700	0.3178
Pathological stage (II vs. I)	1.042	0.523	2.073	0.9078
Degree of differentiation				
Poor vs. Well	0.241	0.032	1.831	0.1692
Moderate vs. Well	0.132	0.016	1.109	0.0622
Degree of inflammation				
Moderate vs. Mild	0.878	0.456	1.690	0.6960
Severe vs. Mild	0.210	0.049	0.906	0.0365
Adjuvant treatment (Yes vs. No)	0.588	0.257	1.342	0.2068
CXCR2 (>20 vs. ≤20)	1.520	0.798	2.894	0.2028

**B**

Covariate	HR	95% CI	P	
Age	1.013	0.984	1.044	0.3825
Sex (M vs. F)	0.884	0.509	1.536	0.6628
Race (White vs. Other)	0.262	0.110	0.625	0.0025
Smoking history				
Former vs. Never	0.424	0.057	3.168	0.4032
Current vs. Never	0.465	0.062	3.483	0.4564
Pathological stage (II vs. I)	1.025	0.567	1.853	0.9352
Degree of differentiation				
Poor vs. Well	0.493	0.067	3.634	0.4876
Moderate vs. Well	0.279	0.035	2.195	0.2252
Degree of inflammation				
Moderate vs. Mild	0.757	0.424	1.351	0.3458
Severe vs. Mild	0.305	0.105	0.883	0.0285
Adjuvant treatment (Yes vs. No)	0.577	0.288	1.156	0.1211
CXCR2 (>20 vs. ≤20)	1.028	0.593	1.782	0.9213

Final multivariate Cox models are presented in Table 2. Combining all patients together, after adjusting for patients' age, sex, and tumor stage, high cytoplasmic CXCR2 expression remained associated with poor overall survival (HR=1.559; 95%CI: 1.051-2.312, P=0.0273) (Table 4A).

**Table 4.** Final multivariate Cox models assessing the effect of covariates on overall survival in the whole population (N=262), in patients with lung adenocarcinoma (N=173) (B), and in patients with lung squamous cell carcinoma (N=89) (C) (M: male; F: female; HR: hazard ratio; 95CI: 95% confidence interval).

**A**

<i>Analysis of Maximum Likelihood Estimates</i>						
<i>Parameter</i>	<i>Parameter Estimate</i>	<i>Standard Error</i>	<i>P-value</i>	<i>HR</i>	<i>95% HR CI</i>	
age	0.02214	0.01048	0.0346	1.022	1.002	1.044
Gender (M vs. F)	0.38869	0.20544	0.0585	1.475	0.986	2.206
Stage (II vs. I)	0.49491	0.22793	0.0299	1.640	1.049	2.564
CXCR2 (>20 vs. <=20)	0.44397	0.20116	0.0273	1.559	1.051	2.312

**B**

<i>Analysis of Maximum Likelihood Estimates</i>						
<i>Parameter</i>	<i>Parameter Estimate</i>	<i>Standard Error</i>	<i>P-value</i>	<i>HR</i>	<i>95% HR CI</i>	
age	0.02064	0.01273	0.1049	1.021	0.996	1.047
Gender (M vs. F)	0.62208	0.25904	0.0163	1.863	1.121	3.095
Stage (II vs. I)	0.72598	0.28779	0.0116	2.067	1.176	3.633
CXCR2 (>20 vs. <=20)	0.34171	0.25741	0.1843	1.407	0.850	2.331

**C**

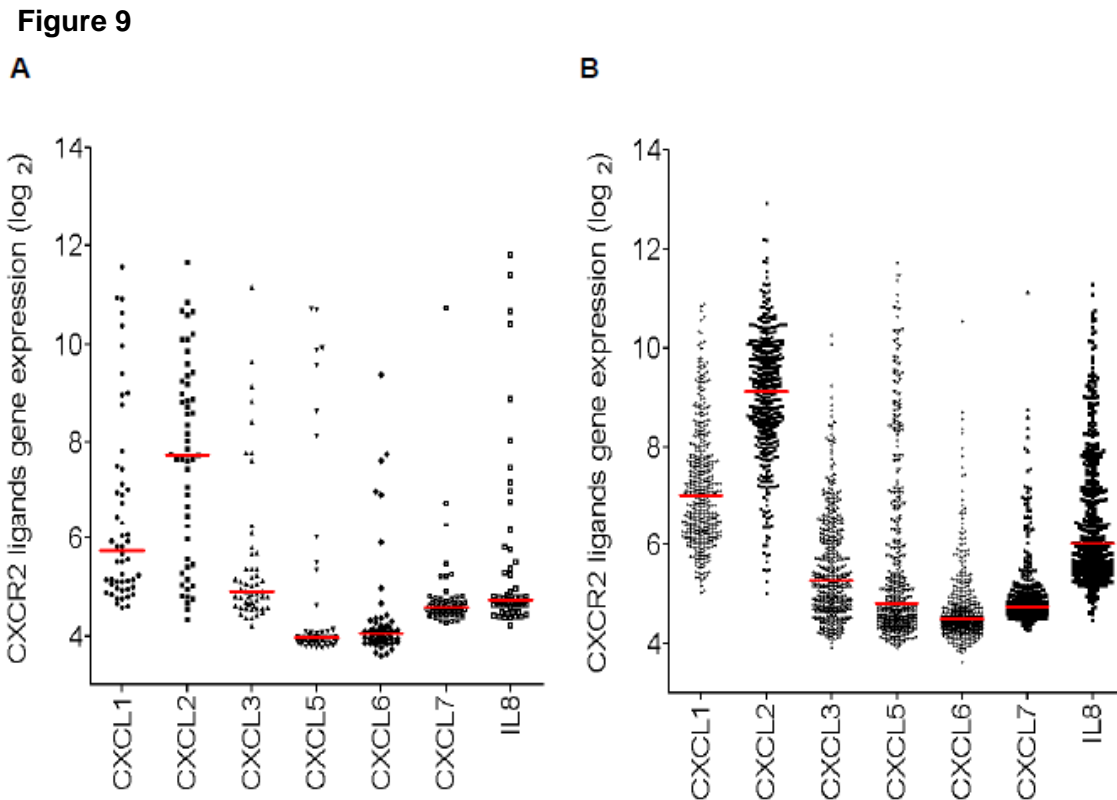
<i>Analysis of Maximum Likelihood Estimates</i>						
<i>Parameter</i>	<i>Parameter Estimate</i>	<i>Standard Error</i>	<i>P-value</i>	<i>HR</i>	<i>95% HR CI</i>	
age	0.02065	0.01939	0.2869	1.021	0.983	1.060
Gender (M vs. F)	0.05144	0.35478	0.8847	1.053	0.525	2.110
Stage (II vs. I)	0.20288	0.39319	0.6059	1.225	0.567	2.647
CXCR2 (>20 vs. <=20)	0.46527	0.33894	0.1698	1.592	0.820	3.094

***Gene expression pattern of CXCR2 axis is associated with human smoking-related adenocarcinoma and adverse clinical features***

High-throughput gene expression profiles offer the opportunity to study CXCR2 as well the genes that encode for its known ligands. We took advantage of publicly available profiles of 52 NSCLC cell lines and 442 early stage resected lung adenocarcinoma. Gene expression patterns of CXCR2 ligands in NSCLC cell lines and lung adenocarcinoma were comparable (Fig. 9). Unsupervised hierarchical clustering using the CXCR2 axis identified a cluster of cell lines with

high expression of CXCR2 ligand genes, which we called the *CXCR2/CXCR2* ligands cluster, that included nine (17%) of the cell lines analyzed (Fig. 9A). This group was enriched in *KRAS* mutations (Fisher's exact test,  $P=0.0548$ ). HCC827, an *EGFR*-mutant cell line with an exon 19 deletion, was also part of this group. In lung adenocarcinomas, a similar cluster of 115 (26%) tumors was identified (Fig. 9B). *EGFR* mutation status was available for 170 adenocarcinomas. None of the 30 tumors included in the *CXCR2/CXCR2* ligands cluster harbored *EGFR* mutations, whereas 24 of the remaining 140 adenocarcinomas did harbor an *EGFR* mutation (Fisher's exact test,  $P=0.0295$ ). A similar *CXCR2/CXCR2* ligands cluster was observed in each of the four individual cohorts forming the DCC (data not shown). From Massarelli E. and Saintigny P., *Cancer Res.* 2013 Jan 15; 73(2):571-82. DOI: 10.1158/0008-5472.

**Figure 9. Distribution of expression of CXCR2, its ligand genes and IL8 in non-small cell lung cancer cell lines and lung adenocarcinomas.** Distribution of expression of *CXCR2* and its ligand genes (*CXCL1*, *CXCL2*, *CXCL3*, *CXCL5*, *CXCL6*, PPBP [*CXCL7*], and *IL8* in non-small cell lung cancer cell lines (panel A; N=52) and lung adenocarcinomas (panel B; N=442).

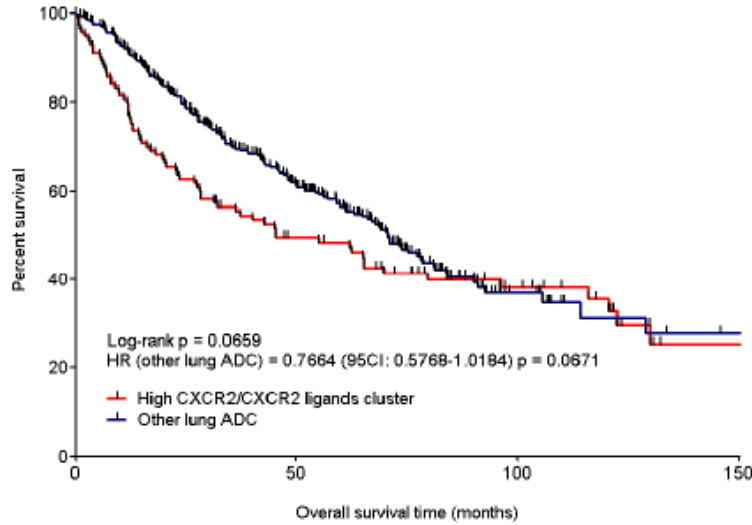


A trend toward a worse prognosis in the high *CXCR2/CXCR2* ligands cluster was observed (Fig. 10A). Using a similar approach in 130 patients resected for squamous cell carcinoma and included in the GEO series GSE4573<sup>54</sup>, we did not see any association between high *CXCR2/CXCR2* ligands cluster and poor outcome (Fig. 10B,C).

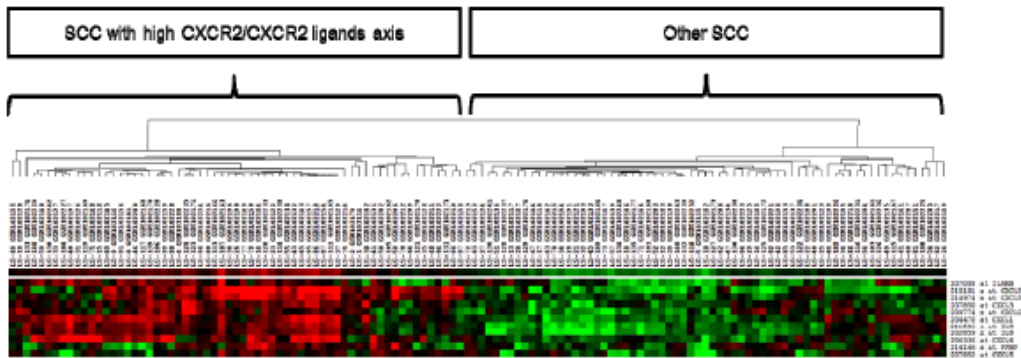
**Figure 10. CXCR2/CXCR2 ligands association with overall survival in patients with lung adenocarcinoma. CXCR2/CXCR2 ligands cluster is associated with a worse overall survival in patients with lung adenocarcinoma (N=442) (A). CXCR2/CXCR2 ligands cluster is not associated with outcome in patients with lung squamous cell carcinoma (N=130) (B, C).**

**Figure 10**

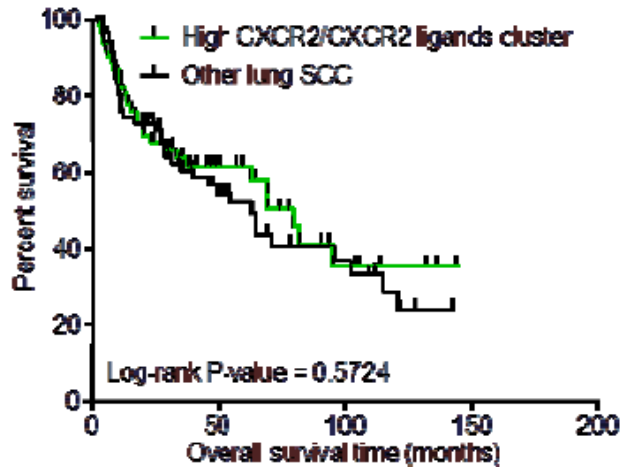
**A**



**B**



**C**

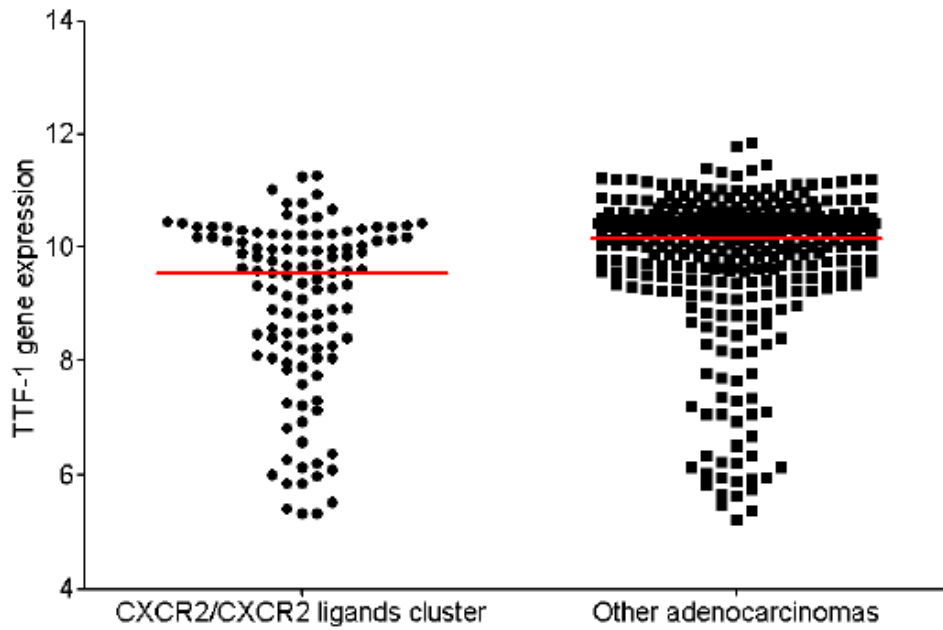


In both cell lines and lung adenocarcinoma, we compared the genes differentially expressed between the *CXCR2/CXCR2* ligands cluster and the remaining samples across the whole genome. In both cases, *CXCL5* gene was the most frequently upregulated in the *CXCR2/CXCR2* ligands cluster. Members of the aldo/keto reductase superfamily (*AKR1B10*, *AKR1C2*, *AKR1C3*), associated with tobacco exposure, were also upregulated. In cell lines, *TGFB1*, vimentin (*VIM*), and osteopontin (*SPP1*) were upregulated in the *CXCR2/CXCR2* ligands cluster, while desmoplakin (*DSP*) and hepatocyte growth factor activator inhibitor 1 (*SPINT1*) were downregulated. These changes may be associated with the epithelial-to-mesenchymal transition and promote invasion and metastasis. In lung adenocarcinomas, genes encoding the matrix metalloproteinases were upregulated in the *CXCR2/CXCR2* ligands cluster, as was the dual specificity phosphatase 4 (*DUSP4*) gene, which is known to be downregulated in *EGFR*-mutant NSCLC. Consistent with the association between poor differentiation and *CXCR2* protein expression observed in the tissue microarray, another striking change was the downregulation of differentiation-associated genes, including thyroid transcription factor 1 (*NKX2-1*) (Fig. 11A) and surfactant proteins B (*SFTPB*), C (*SFTPC*), and D (*SFTPD*), in the *CXCR2/CXCR2* ligands cluster. Interestingly, ribonucleotide reductase M2 (*RRM2*) was upregulated in the *CXCR2/CXCR2* ligands cluster, while folic acid receptor 1 (*FOLR1*) was downregulated. *RRM2* and *FOLR1* have been reported to modulate response to gemcitabine and pemetrexed, respectively, in NSCLC. Similar trends were observed in cell lines for *FOLR1* and *NKX2-1* downregulation (Fig. 11B).

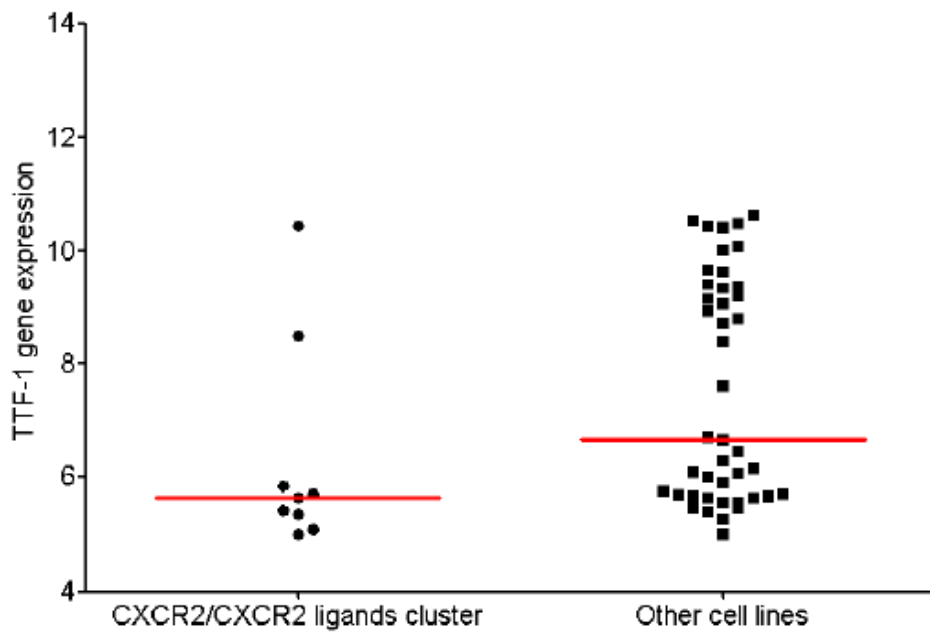
**Figure 11. *TTF-1* gene expression in lung adenocarcinomas and cell lines.** *TTF-1* gene expression was more frequently lower in lung adenocarcinomas (A) and cell lines (B) included in the *CXCR2/CXCR2* ligands cluster.

**Figure 11**

**A**



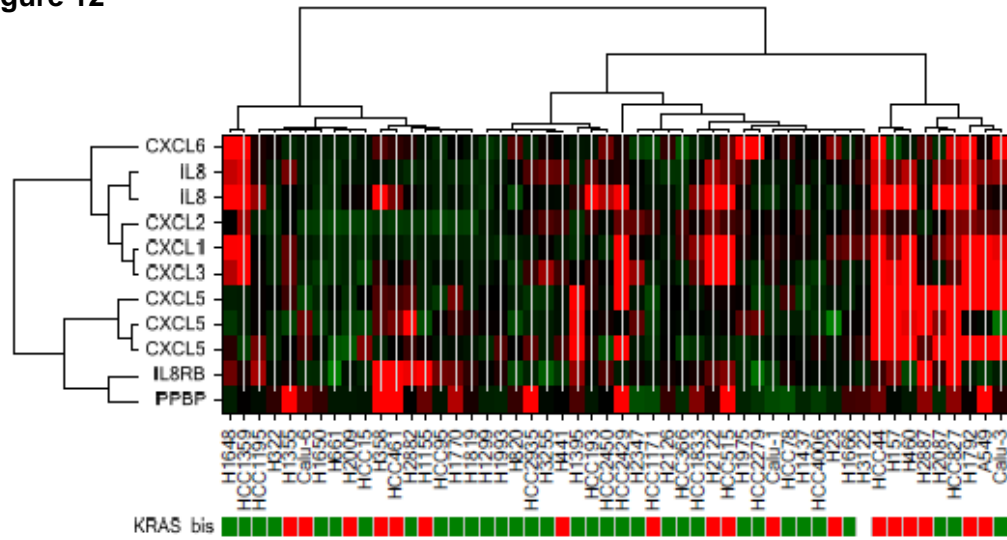
**B**



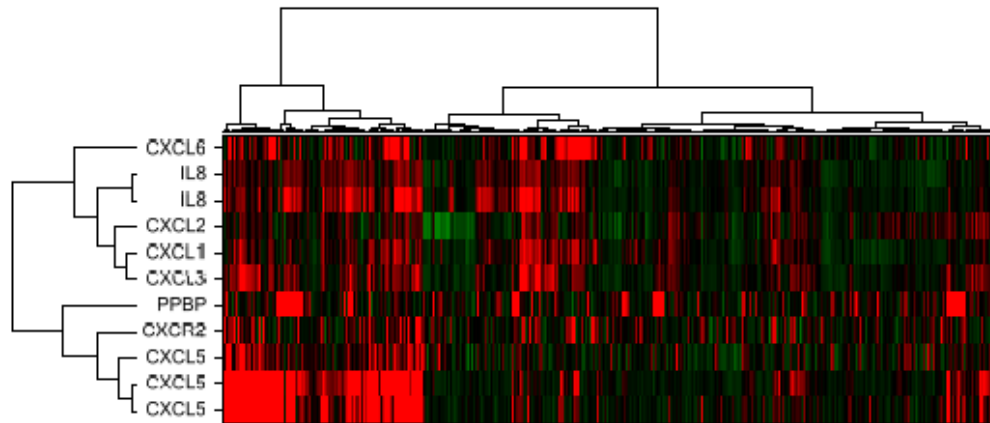
The most significant network associated with differential gene expression, with an absolute fold-change  $\geq 0.5$  between the *CXCR2/CXCR2* ligands cluster and the remaining samples, was related to *NFKB* in both the cell lines and lung adenocarcinoma (data not shown). Using as input the fold-change in gene expression between the *CXCR2/CXCR2* ligands cluster and the remaining lung adenocarcinomas, GSEA showed enrichment of genes associated with poor survival (Fig. 12C) (28). We also found enrichment in gene sets associated with poor differentiation and proliferation (data not shown), as well as MET transcriptionally co-regulated genes (Fig. 12D). Using as input the fold-change in gene expression between the *CXCR2/CXCR2* ligands cluster and the remaining cell lines, GSEA showed a significant upregulation of gene sets related to the RAS pathway (Fig. 12E) and resistance to gefitinib (Fig. 12F), and enrichment of target genes of hsa-miR-let7, a known regulator of *KRAS* expression, and of genes associated with the epithelial-to-mesenchymal transition was observed (data not shown).

**Figure 12. Identification of a *CXCR2/CXCR2* ligands cluster.** Unsupervised clustering using gene expression of *CXCR2* and its ligands (*CXCL6*, *IL8*, *CXCL2*, *CXCL1*, *CXCL3*, *PPBP* [*CXCL7*], and *CXCL5*) in (A) 52 NSCLC cell lines and (B) 442 lung adenocarcinomas. For Gene Set Enrichment Analysis, genes were preranked according to the fold-change observed between samples with the *CXCR2/CXCR2* ligands cluster and the remaining samples in both lung adenocarcinomas (C, D) and cell lines (E, F); representative gene sets enriched with a *P*-value and a false discovery rate  $< 0.0001$  are shown for lung adenocarcinomas (C, D) and NSCLC cell lines (E, F).

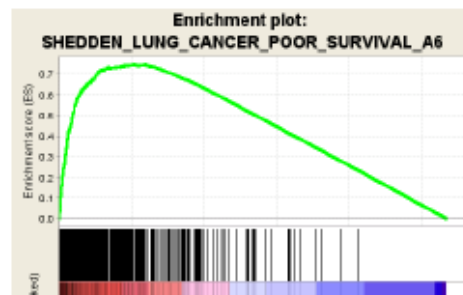
**Figure 12**  
**A**



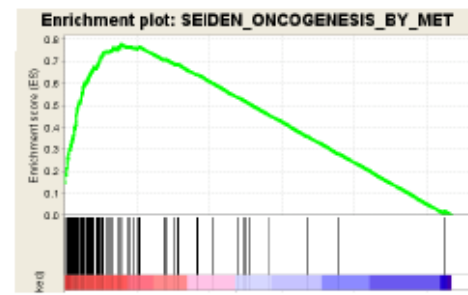
**B**



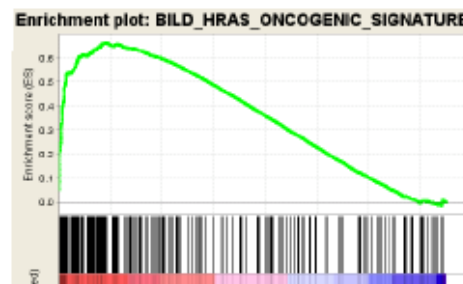
**C**



**D**



**E**



**F**

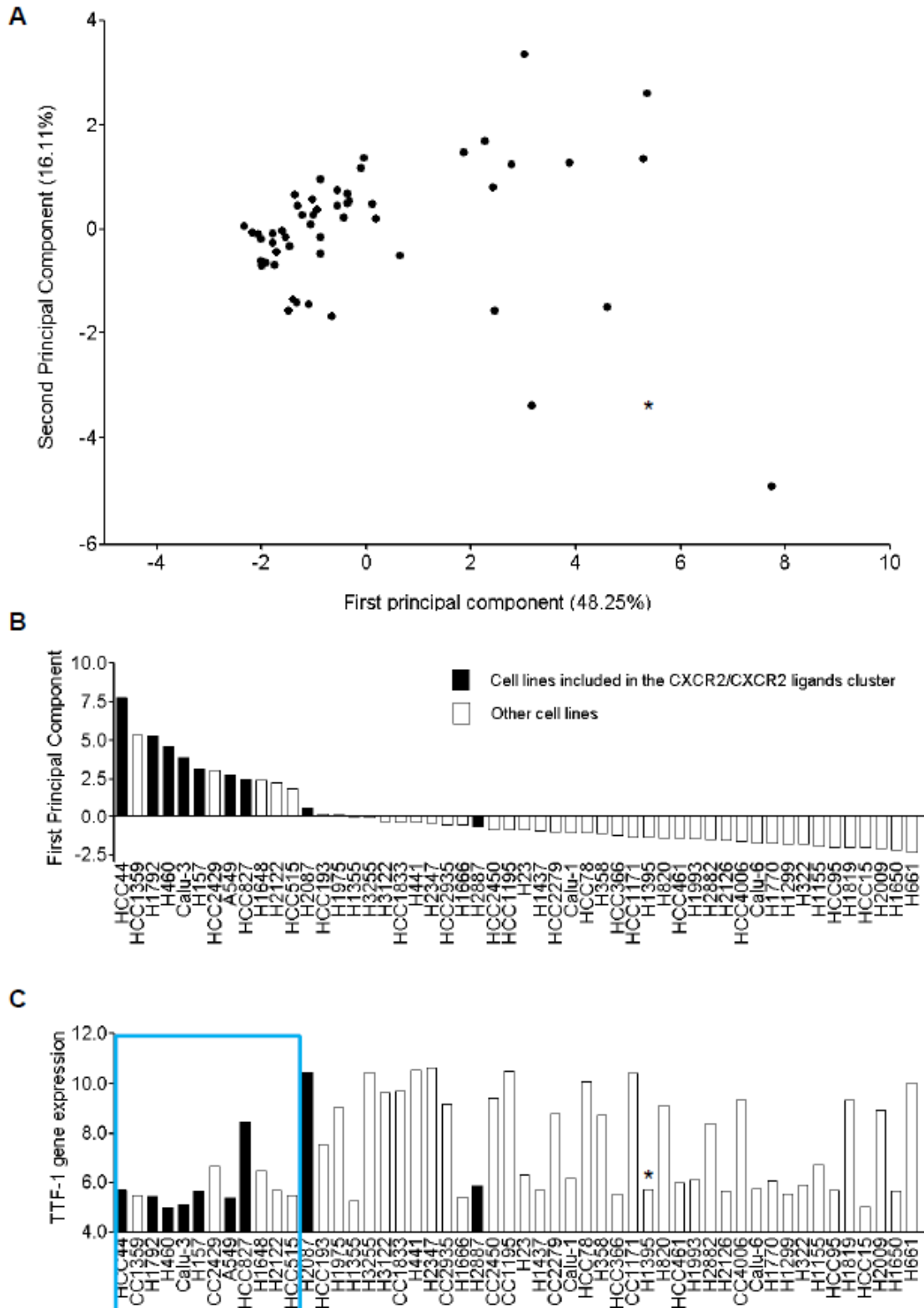




As an alternative approach to studying the effect of the *CXCR2/CXCR2* ligands axis, we summarized the effect of this axis by computing a principal components analysis (Fig. 13A and 14A). The distribution of PC1 in cell lines was bimodal, a group of 12 cell lines having a high PC1 ( $\geq 1.5$ ) and the remaining cell lines having a low PC1 (Fig. 13B). Interestingly, cell line H1395, which has been reported to harbor an inactivating *CXCR2* G354W mutation, had a low PC1 (Fig. 13B). Cell lines included in the *CXCR2/CXCR2* ligands cluster or with a high PC1 had low levels of *NKX2-1* gene expression, except HCC827 (Fig. 13C).

**Figure 13. Expression of *CXCR2* and its ligand genes in NSCLC cell lines.** The first two principal components were computed using expression of *CXCR2* and its ligand genes (*CXCL1*, *CXCL2*, *CXCL3*, *CXCL5*, *CXCL6*, *PPBP* [*CXCL7*], and *IL8*) in 52 NSCLC cell lines. (A) The first principal component (PC1) accounted for 48.25% of the variation of the principal components analysis and allowed identification of two groups of cell lines (bimodal distribution). (B) Cell lines with a high PC1 had a significant overlap with cell lines included in the *CXCR2/CXCR2* ligands cluster. (C) *TTF-1* gene expression was low in almost all the cell lines with high PC1 outlined by the blue box. NCI-H1395 (shown by a star) has an inactivating *CXCR2* G354W mutation.

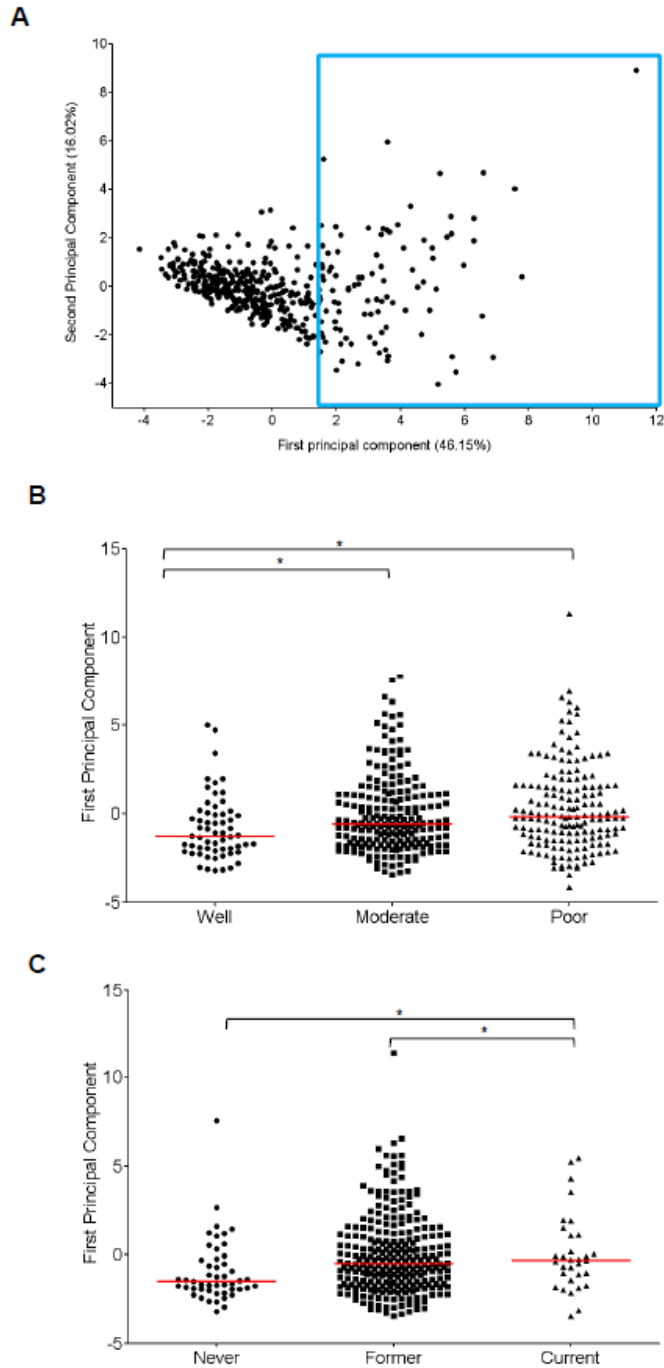
**Figure 13**



In lung adenocarcinomas, a similar bimodal distribution of PC1 was observed (Fig. 14A). Consistently with our immunohistochemical results, PC1 was statistically significantly higher in poorly differentiated adenocarcinomas than in moderately ( $P=0.0065$ ) and well-differentiated tumors ( $P=0.0006$ ) (Fig. 14B), and higher in current smokers than in former ( $P=0.0010$ ) and never smokers ( $P=0.0085$ ) (Fig.14C).

**Figure 14. Expression of *CXCR2* and its ligand genes in lung adenocarcinomas.** The first two principal components were computed using expression of *CXCR2* and its ligand genes (*CXCL1*, *CXCL2*, *CXCL3*, *CXCL5*, *CXCL6*, *PPBP* [*CXCL7*], and *IL8*) in 444 lung adenocarcinomas. (A) The first principal component (PC1) accounted for 46.15% of the variation of the principal component analysis in lung adenocarcinomas. (B) PC1 was statistically higher in poorly differentiated versus moderately ( $P=0.0065$ ) or well differentiated ( $P=0.0006$ ) lung adenocarcinomas and (C) in current versus former ( $P=0.0010$ ) or never smokers  $P=0.0085$ .

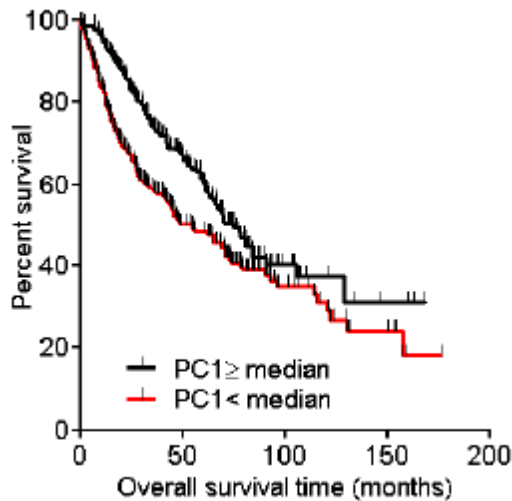
**Figure 14**



When PC1 was dichotomized based on the median, tumors with low PC1 linked with longer OS (Fig. 15); low PC1 was associated with HR of 0.6907 (95CI: 0.5302-0.9000,  $P$ value= 0.0061). After adjusting for patient age, sex, tumor stage, and institution, low PC1 remained associated with longer overall survival (HR of 0.6827; 95CI: 0.5046-0.8701,  $P$ =0.0031) (Fig 15).

**Figure 15. PC1 and overall survival.**

**Figure 15**

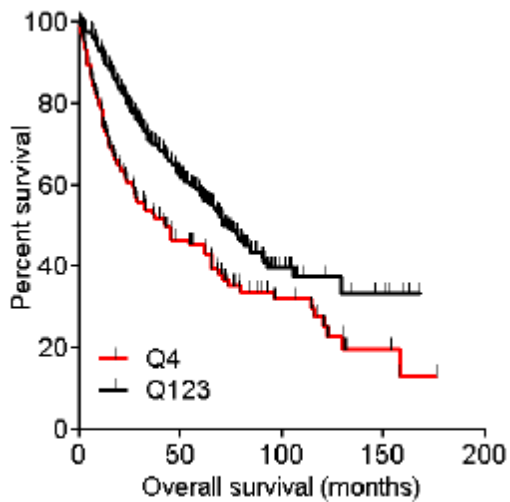


***CXCL5 is the main driver of the CXCR2/CXCR2 ligands cluster in adenocarcinomas and is regulated through promoter methylation***

*CXCL5* was the gene most upregulated in the *CXCR2/CXCR2* ligands cluster in comparison to other samples across the whole genome, in both the cell lines and lung adenocarcinomas. *CXCL5* upregulation was associated with poor overall survival (Fig. 16).

**Figure 16. CXCL5 upregulation and overall survival.**

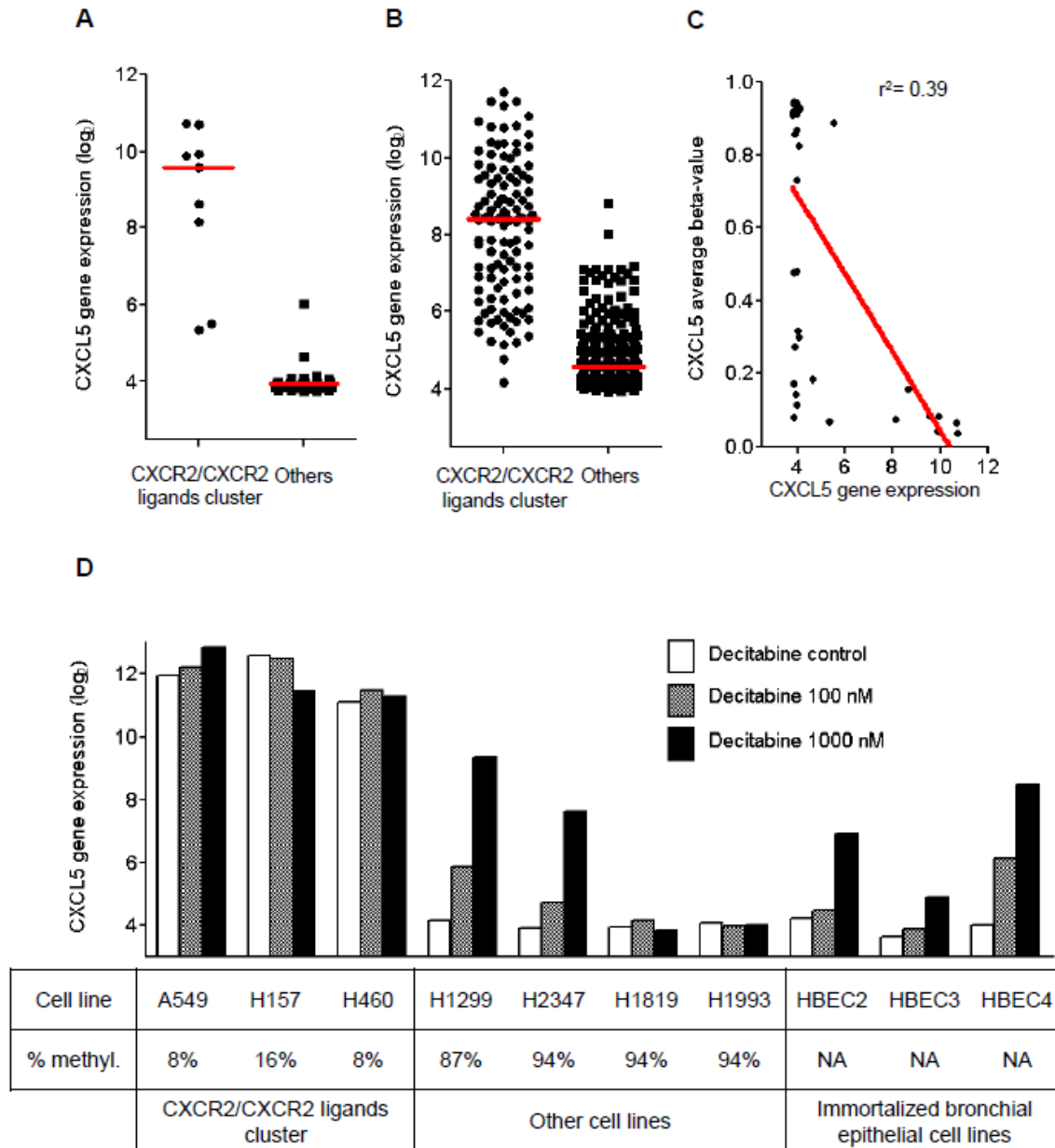
**Figure 16**



Its distribution was bimodal in both cell lines and lung adenocarcinomas (Fig. 17A and B). This led us to hypothesize that promoter methylation might regulate its expression. *CXCL5* gene expression was inversely correlated with the average beta-value, which measures the degree of methylation of the promoter (Fig. 17C). Data generated in an independent study with publicly available raw data<sup>55</sup> confirmed high levels of expression of *CXCL5* in cell lines included in the *CXCR2/CXCR2* ligands axis, and low levels in other cell lines, including immortalized HBEC lines (Fig. 17D).

**Figure 17. CXCL5 drives the CXCR2/CXCR2 ligands cluster and is regulated through promoter methylation.** CXCL5 is the gene most frequently upregulated across the whole genome in samples with the CXCR2/CXCR2 ligands cluster compared to other samples, both *in vitro* (A) and *in vivo* (B). (C) CXCL5 gene expression was inversely correlated with the average beta-value, and (D) was increased after treatment with decitabine in most of the cell lines with low baseline CXCL5 expression.

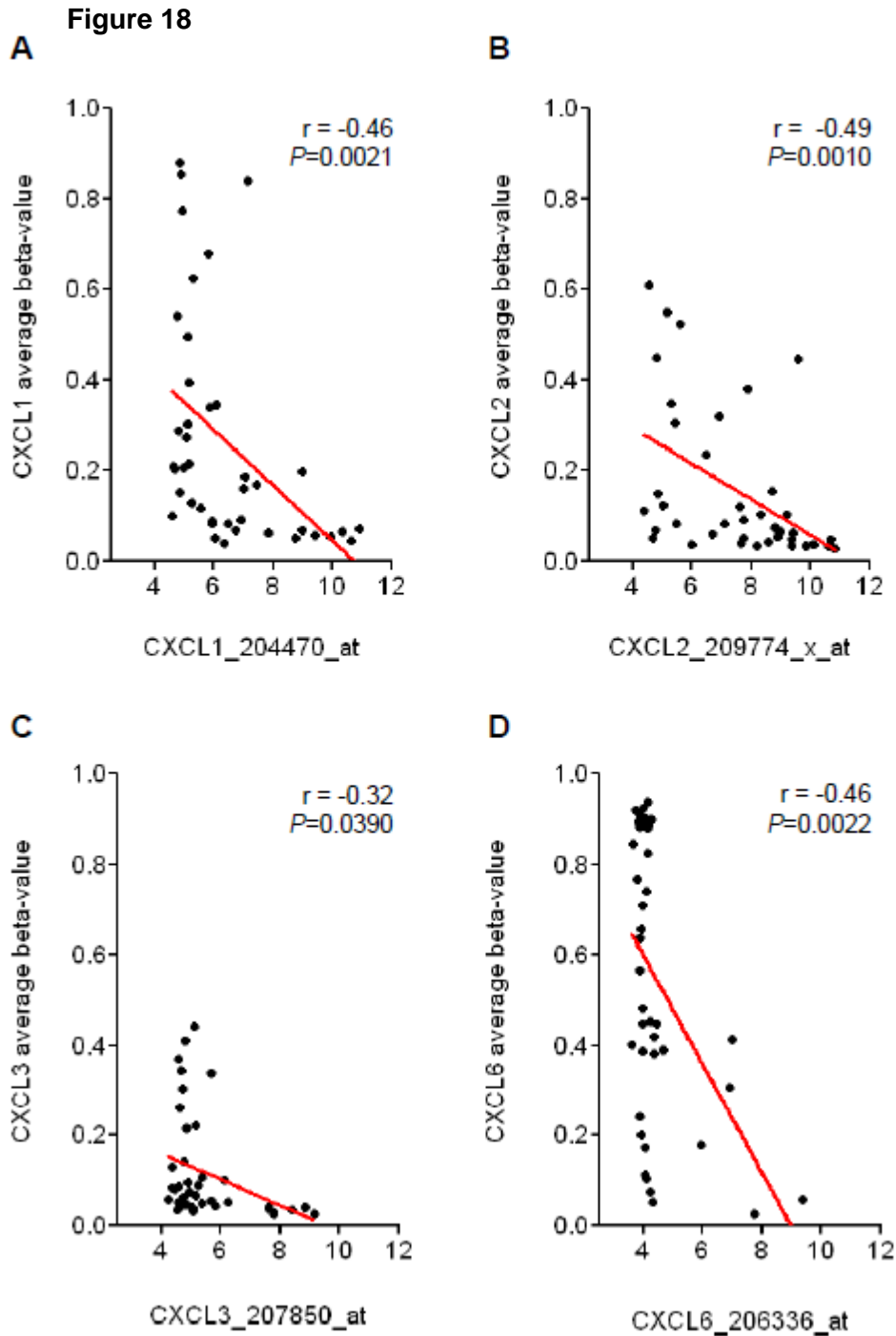
**Figure 17**



Moreover, *CXCL5* expression was induced by decitabine in most of the cell lines with low *CXCL5* expression that were shown to be methylated, as well as in HBEC cells. Expression of *CXCL1* ( $r = -0.46$ ,  $P=0.0021$ ), *CXCL2* ( $r = -0.49$ ,  $P=0.0010$ ), *CXCL3* ( $r = -0.32$ ,  $P=0.0390$ ), and *CXCL6* ( $r = -0.46$ ,  $P=0.0022$ ) genes was significantly inversely correlated with the average beta-value of their respective promoter, suggesting regulation through promoter methylation (Fig. 18A-D).



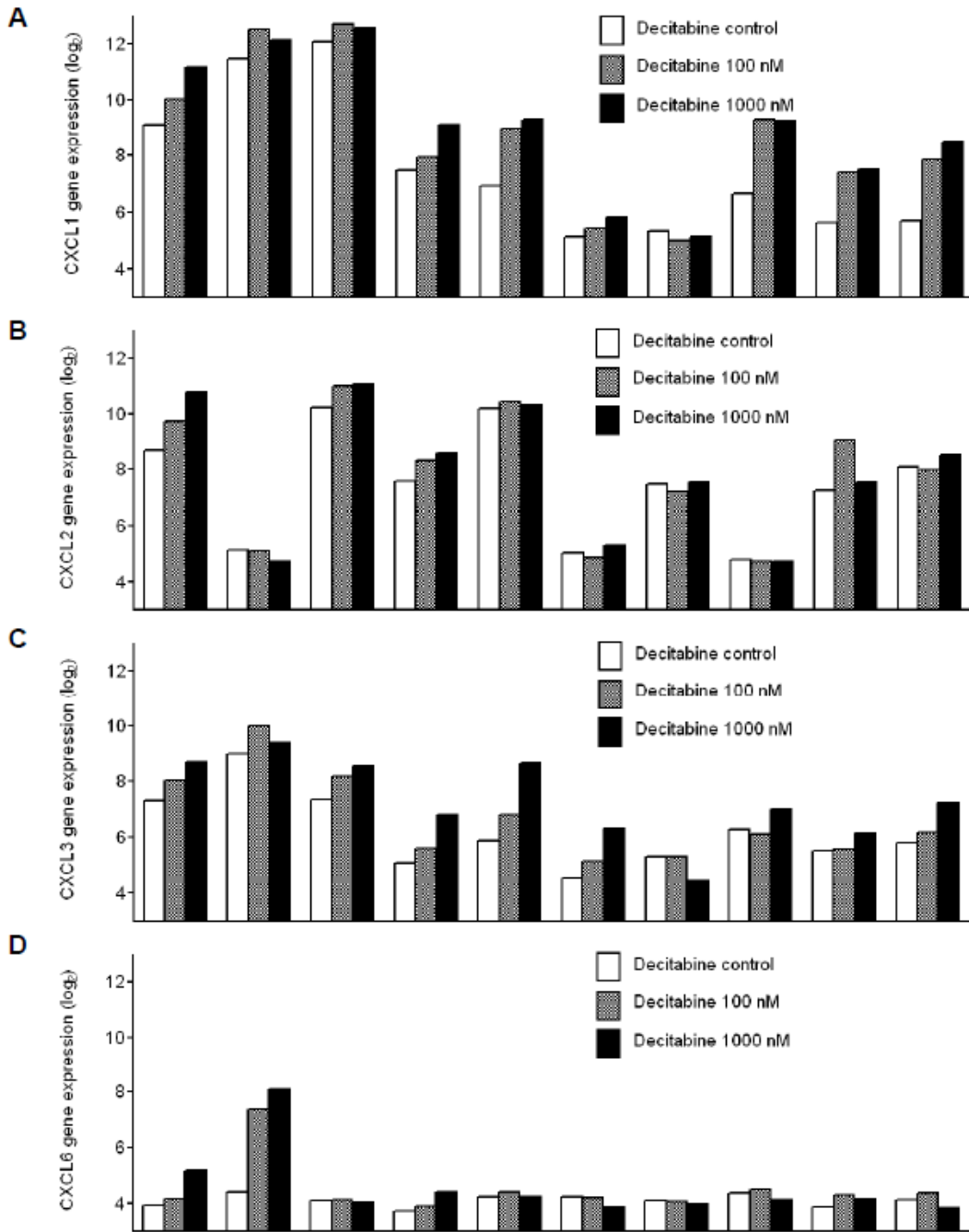
**Figure 18. Promoter methylation of CXCR2 ligand genes.** Expression of (A) *CXCL1*, (B) *CXCL2*, (C) *CXCL3*, and (D) *CXCL6* genes was negatively correlated with the level of their promoter methylation as indicated by average beta-value.



However, only *CXCL1* and *CXCL3* had patterns similar to *CXCL5* in terms of response to decitabine (Fig. 19A-D).

**Figure 19. Effect of decitabine on CXCR2 ligand genes.** The effect of two doses of decitabine on (A) *CXCL1*, (B) *CXCL2*, (C) *CXCL3*, and (D) *CXCL6* gene expression levels in 10 lung cell lines is shown.

**Figure 19**



Cell line	A549	H157	H460	H1299	H2347	H1819	H1993	HBEC2	HBEC3	HBEC4
	CXCR2/CXCR2 ligands cluster			Other cell lines				Immortalized bronchial epithelial cell lines		

## DISCUSSION

We show that *in vivo* CXCR2 inhibition by knock-down in a murine cell line (344SQ), which has a known high metastatic potential, reduces its invasive ability. In a murine model of orthotopic syngeneic lung adenocarcinoma CXCR2 knock-down 344SQ cell line was found to be associated with decreased tumor burden, local and distant metastases. In order to translate our preclinical discoveries to human NSCLC, we explored CXCR2 tumoral immunohistochemical expression in tissue microarrays from patients with surgically resected stage I-II lung adenocarcinoma and correlated it with patient clinic-pathological characteristics including smoking status, histological differentiation and survival outcomes. We considered also localization of CXCR2 expression in the cytoplasm, membrane and nucleus. High cytoplasmic CXCR2 was associated with smoking history, aggressive histological differentiation and worse survival. When we screened a publicly available large database of NSCLC cell lines and lung adenocarcinomas, we found that at the gene expression level, CXCL5, a CXCR2-ligand, was the main driver of a cluster of cell lines and lung adenocarcinomas with high-risk features, including *RAS* and *MET* pathway activation, epithelial-to-mesenchymal transition and resistance to epidermal growth factor inhibition (i.e., gefitinib). We have named this CXCR2/CXCR2 ligands cluster and we discovered that CXCL5 in this cluster was regulated by promoter methylation.

Several studies have reported a critical role of CXCR2 inhibition in melanoma<sup>43; 59</sup>, ovarian<sup>59</sup>, prostate<sup>60</sup>, and esophageal cancers<sup>61</sup> mainly by regulating the cell cycle, apoptosis and angiogenesis via multiple signaling pathways including PI3K/AKT, NF- $\kappa$ B, MAPK and STAT3. However, there is not a clear understanding if CXCR2 inhibition plays a direct effect on tumoral cells. We have tested our hypothesis using a novel orthotopic syngeneic lung cancer metastasis model with preserved immunity via

injection of a highly metastatic cell line (344SQ) derived from *Kras*<sup>LA1/+</sup>*p53*<sup>R172HΔG/+</sup> mice. This murine model reliably represents the developmental process of human lung adenocarcinomas<sup>29</sup>. The effect of CXCR2 knock-down in shRNA stable clones on the substantial reduction of the thoracic tumors, lymphatic and distant metastases, is unlikely due to regulation of angiogenesis. In fact, data published showing the effect of CXCR2 knockdown in ovarian cancer cell lines on decreasing tumor angiogenesis by VEGF activation, were obtained using immunosuppressed murine xenografts tumor models which do not take into consideration the interaction between the tumoral cells and the tumor microenvironment<sup>62</sup>. We understand that our work lacks of a direct evaluation on tumor angiogenesis, therefore, we cannot completely rule out a direct effect of CXCR2 knockdown in the 344SQ cells on tumor angiogenesis.

When we explored in human NSCLC samples the tumoral cell localization of CXCR2 by IHC, we observed that only cytoplasmic expression was associated with significant difference in terms of smoking history, histologic differentiation and survival. Although many chemokine receptors internalize through clathrin-coated pits, regulation of the receptor trafficking is not fully understood. Fan GH et al. showed colocalization of CXCR2 with transferrin and low-density lipoprotein (LDL) after agonist treatment for different periods of time, suggesting 2 intracellular trafficking pathways for this receptor. CXCR2 was colocalized with Rab5 and Rab11a, which are localized in early and recycling endosomes, respectively, in response to agonist stimulation for a short period of time, suggesting a recycling pathway for the receptor trafficking<sup>63</sup>. The altered distribution of CXCR2 into the cytoplasm may start an autocrine loop that may contribute as a transcriptional signaling to augment expression of receptor-ligand production as previously suggested in prostate cancer progression<sup>60</sup>.

CXCR2 inhibition has been reported to also affect the epithelial to-mesenchymal transition via abrogation of the Snail-mediated increase in tumor burden in murine models of NSCLC<sup>39; 64</sup>. However, contrasting results were described on this topic in a small cohort of 20 NSCLC showing a correlation between CXCR2 expression and improved survival<sup>65</sup>. In addition, a role of *CXCR2* as tumor suppressor gene was also underscored in studies about tumor senescence and response to oncogenic signals<sup>66</sup>. Our GSEA analysis results show that c-MET oncogenic pathway is expressed in the *CXCR2/CXCR2* ligands cluster, which is in line with the observation of downregulation of *SPINT1*, a potent inhibitor specific for HGF activator, and upregulation of *TGFB1* and *VIM* in the *CXCR2/CXCR2* ligands cluster<sup>67</sup>.

Another interesting finding of our tissue microarray and GSEA analysis was the association of CXCR2 protein expression, the *CXCR2/CXCR2* ligands cluster and high histological grade. The thyroid transcription factor 1 (*TTF1, NKX2-1*), which is a lineage survival gene abnormally expressed in about 70% of lung adenocarcinoma, was one of the genes most frequently downregulated in the cluster compared to other lung adenocarcinomas. Interestingly, NKX2-1 protein expression in human NSCLC has been reported in the literature to be prevalent in lung adenocarcinoma, female gender, non-smoking history, presence of epidermal growth factor receptor (EGFR) mutation and better overall survival and it is one of the routinely tested immunohistochemical markers for the pathological diagnosis of NSCLC<sup>68</sup>. Absence of NKX2-1 expression may identify lung adenocarcinomas with CXCR2 activation, with interesting repercussion on the identification of tumors which may be targeted by CXCR2 inhibition. In addition, the correlation between NKX2-1 protein expression and presence of epidermal growth factor receptor (*EGFR*) mutation, is in line with the findings of absence of *EGFR* mutations in the lung adenocarcinoma included in the

*CXCR2/CXCR2* ligands cluster in the DCC dataset which doesn't express NKX2-1 protein. Our findings in the DCC dataset also highlight the association of *CXCR2* expression and *KRAS* mutation which is indication of EGFR tyrosine kinase inhibitor therapy resistance<sup>69</sup>. These observations are in line with the strong inhibitory effect of *CXCR2* knockdown in our orthotopic syngeneic lung adenocarcinoma metastasis model, which harbors a *KRAS* mutation. Therefore, *CXCR2* may represent an important target of *KRAS*-driven lung adenocarcinomas.

The findings of *CXCL5* being the main driver gene in the *CXCR2/CXCR2* ligands cluster add to the current literature where there are controversial reports about its significance in different tumor types. In head and neck squamous cell carcinoma *CXCL5* has been associated with tumor cell proliferation, migration and invasion<sup>70</sup>. On the other hand, knock down cell clones of colon carcinoma resulted in a rapid tumor growth and in a number of tumor metastases *in vivo*<sup>71</sup>. In the same study low expression of *CXCL5* by immunohistochemistry was significantly associated with poor outcome in human colon cancer patients<sup>71</sup>. In human lung adenocarcinoma there is no data on the association of *CXCL5* expression and prognosis. However, in NSCLC methylation appears the main mechanism of regulation<sup>72</sup>. We found that about 75-80% of NSCLC harbor *CXCL5* promoter methylation with sub sequential silencing of the gene. These observations may suggest that *CXCL5* might promote tumorigenesis in 20% of lung adenocarcinomas through *CXCR2* autocrine and paracrine loop.

In conclusion, our data show that tumoral *CXCR2* inhibition has an important role on regulation of invasion, growth *in vitro* and *in vivo* in an orthotopic syngeneic lung adenocarcinoma metastasis model with *KRAS* and *TP53* mutations. We identified a cluster of human NSCLC cell lines and lung adenocarcinomas, in which prognosis seems to be affected by the *CXCR2-CXCL5* axis with an interesting association to aggressive histology and smoking history. Pharmaceutical inhibition of *CXCR2* is

currently undergoing clinical development in COPD to counter-act the damaging effects of cigarette smoking that produces inflammation with increase in alveolar destruction by neutrophils, goblet cell hyperplasia and pro-angiogenic effects<sup>17; 44</sup>. In addition, the finding of a cluster of lung adenocarcinomas with CXCR-2 ligand overexpression may be of great value in directing novel approaches in T cell adoptive therapy of lung cancer, as showed by Peng W. et al, who introduced the *CXCR2* gene into tumor-specific T cells to enhance their localization to tumors and improve antitumor immune responses<sup>73</sup>. Therefore, with the future availability of CXCR2 targeted therapy in clinical cancer research, CXCR2 expression may become an interesting target to validate in prospective clinical trials in NSCLC.

## BIBLIOGRAPHY

1. Siegel, R., Naishadham, D. & Jemal, A. (2013). Cancer statistics, 2013. *CA Cancer J Clin* 63, 11-30.
2. Travis, W. D., Brambilla, E., Noguchi, M., Nicholson, A. G., Geisinger, K. R., Yatabe, Y., Beer, D. G., Powell, C. A., Riely, G. J., Van Schil, P. E., Garg, K., Austin, J. H., Asamura, H., Rusch, V. W., Hirsch, F. R., Scagliotti, G., Mitsudomi, T., Huber, R. M., Ishikawa, Y., Jett, J., Sanchez-Cespedes, M., Sculier, J. P., Takahashi, T., Tsuboi, M., Vansteenkiste, J., Wistuba, I., Yang, P. C., Aberle, D., Brambilla, C., Flieder, D., Franklin, W., Gazdar, A., Gould, M., Hasleton, P., Henderson, D., Johnson, B., Johnson, D., Kerr, K., Kuriyama, K., Lee, J. S., Miller, V. A., Petersen, I., Roggli, V., Rosell, R., Saijo, N., Thunnissen, E., Tsao, M. & Yankelewitz, D. (2011). International association for the study of lung cancer/american thoracic society/european respiratory society international multidisciplinary classification of lung adenocarcinoma. *J Thorac Oncol* 6, 244-85.
3. Schiller, J. H., Harrington, D., Belani, C. P., Langer, C., Sandler, A., Krook, J., Zhu, J. & Johnson, D. H. (2002). Comparison of four chemotherapy regimens for advanced non-small-cell lung cancer. *N Engl J Med* 346, 92-8.
4. Scagliotti, G. V., Parikh, P., von Pawel, J., Biesma, B., Vansteenkiste, J., Manegold, C., Serwatowski, P., Gatzemeier, U., Digumarti, R., Zukin, M., Lee, J. S., Mellemaard, A., Park, K., Patil, S., Rolski, J., Goksel, T., de Marinis, F., Simms, L., Sugarman, K. P. & Gandara, D. (2008). Phase III study comparing cisplatin plus gemcitabine with cisplatin plus pemetrexed in chemotherapy-naive



- patients with advanced-stage non-small-cell lung cancer. *J Clin Oncol* 26, 3543-51.
5. Lynch, T. J., Bell, D. W., Sordella, R., Gurubhagavatula, S., Okimoto, R. A., Brannigan, B. W., Harris, P. L., Haserlat, S. M., Supko, J. G., Haluska, F. G., Louis, D. N., Christiani, D. C., Settleman, J. & Haber, D. A. (2004). Activating mutations in the epidermal growth factor receptor underlying responsiveness of non-small-cell lung cancer to gefitinib. *N Engl J Med* 350, 2129-39.
  6. Paez, J. G., Janne, P. A., Lee, J. C., Tracy, S., Greulich, H., Gabriel, S., Herman, P., Kaye, F. J., Lindeman, N., Boggon, T. J., Naoki, K., Sasaki, H., Fujii, Y., Eck, M. J., Sellers, W. R., Johnson, B. E. & Meyerson, M. (2004). EGFR mutations in lung cancer: correlation with clinical response to gefitinib therapy. *Science* 304, 1497-500.
  7. Soda, M., Choi, Y. L., Enomoto, M., Takada, S., Yamashita, Y., Ishikawa, S., Fujiwara, S., Watanabe, H., Kurashina, K., Hatanaka, H., Bando, M., Ohno, S., Ishikawa, Y., Aburatani, H., Niki, T., Sohara, Y., Sugiyama, Y. & Mano, H. (2007). Identification of the transforming EML4-ALK fusion gene in non-small-cell lung cancer. *Nature* 448, 561-6.
  8. Suda, K., Tomizawa, K., Yatabe, Y. & Mitsudomi, T. (2011). Lung cancers unrelated to smoking: characterized by single oncogene addiction? *Int J Clin Oncol* 16, 294-305.
  9. Weinstein, I. B. (2002). Cancer. Addiction to oncogenes--the Achilles heel of cancer. *Science* 297, 63-4.
  10. Pao, W. & Girard, N. (2011). New driver mutations in non-small-cell lung cancer. *Lancet Oncol* 12, 175-80.

11. Paik, P. K., Arcila, M. E., Fara, M., Sima, C. S., Miller, V. A., Kris, M. G., Ladanyi, M. & Riely, G. J. (2011). Clinical characteristics of patients with lung adenocarcinomas harboring BRAF mutations. *J Clin Oncol* 29, 2046-51.
12. Le, Y., Zhou, Y., Iribarren, P. & Wang, J. (2004). Chemokines and chemokine receptors: their manifold roles in homeostasis and disease. *Cell Mol Immunol* 1, 95-104.
13. Schadendorf, D., Moller, A., Algermissen, B., Worm, M., Sticherling, M. & Czarnecki, B. M. (1993). IL-8 produced by human malignant melanoma cells in vitro is an essential autocrine growth factor. *J Immunol* 151, 2667-75.
14. Zhu, Y. M., Webster, S. J., Flower, D. & Woll, P. J. (2004). Interleukin-8/CXCL8 is a growth factor for human lung cancer cells. *Br J Cancer* 91, 1970-6.
15. Wang, J. M., Taraboletti, G., Matsushima, K., Van Damme, J. & Mantovani, A. (1990). Induction of haptotactic migration of melanoma cells by neutrophil activating protein/interleukin-8. *Biochem Biophys Res Commun* 169, 165-70.
16. Balkwill, F. (2004). Cancer and the chemokine network. *Nat Rev Cancer* 4, 540-50.
17. Chapman, R. W., Phillips, J. E., Hipkin, R. W., Curran, A. K., Lundell, D. & Fine, J. S. (2009). CXCR2 antagonists for the treatment of pulmonary disease. *Pharmacol Ther* 121, 55-68.
18. Strieter, R. M., Poverini, P. J., Kunkel, S. L., Arenberg, D. A., Burdick, M. D., Kasper, J., Dzuiba, J., Van Damme, J., Walz, A., Marriott, D. & et al. (1995). The functional role of the ELR motif in CXC chemokine-mediated angiogenesis. *J Biol Chem* 270, 27348-57.
19. Addison, C. L., Daniel, T. O., Burdick, M. D., Liu, H., Ehlert, J. E., Xue, Y. Y., Buechi, L., Walz, A., Richmond, A. & Strieter, R. M. (2000). The CXC chemokine

- receptor 2, CXCR2, is the putative receptor for ELR+ CXC chemokine-induced angiogenic activity. *J Immunol* 165, 5269-77.
20. Keane, M. P., Belperio, J. A., Xue, Y. Y., Burdick, M. D. & Strieter, R. M. (2004). Depletion of CXCR2 inhibits tumor growth and angiogenesis in a murine model of lung cancer. *J Immunol* 172, 2853-60.
  21. Heidemann, J., Ogawa, H., Dwinell, M. B., Rafiee, P., Maaser, C., Gockel, H. R., Otterson, M. F., Ota, D. M., Lugerling, N., Domschke, W. & Binion, D. G. (2003). Angiogenic effects of interleukin 8 (CXCL8) in human intestinal microvascular endothelial cells are mediated by CXCR2. *J Biol Chem* 278, 8508-15.
  22. Belperio, J. A., Keane, M. P., Burdick, M. D., Gomperts, B., Xue, Y. Y., Hong, K., Mestas, J., Ardehali, A., Mehrad, B., Saggari, R., Lynch, J. P., Ross, D. J. & Strieter, R. M. (2005). Role of CXCR2/CXCR2 ligands in vascular remodeling during bronchiolitis obliterans syndrome. *J Clin Invest* 115, 1150-62.
  23. Murdoch, C. & Finn, A. (2000). Chemokine receptors and their role in inflammation and infectious diseases. *Blood* 95, 3032-43.
  24. Wang, S., Yue, H., Derin, R. B., Guggino, W. B. & Li, M. (2000). Accessory protein facilitated CFTR-CFTR interaction, a molecular mechanism to potentiate the chloride channel activity. *Cell* 103, 169-79.
  25. Wu, Y., Wang, S., Farooq, S. M., Castelveter, M. P., Hou, Y., Gao, J. L., Navarro, J. V., Oupicky, D., Sun, F. & Li, C. (2012). A chemokine receptor CXCR2 macromolecular complex regulates neutrophil functions in inflammatory diseases. *J Biol Chem* 287, 5744-55.
  26. Chen, J. J., Yao, P. L., Yuan, A., Hong, T. M., Shun, C. T., Kuo, M. L., Lee, Y. C. & Yang, P. C. (2003). Up-regulation of tumor interleukin-8 expression by infiltrating macrophages: its correlation with tumor angiogenesis and patient survival in non-small cell lung cancer. *Clin Cancer Res* 9, 729-37.

27. White, E. S., Flaherty, K. R., Carskadon, S., Brant, A., Iannettoni, M. D., Yee, J., Orringer, M. B. & Arenberg, D. A. (2003). Macrophage migration inhibitory factor and CXCL chemokine expression in non-small cell lung cancer: role in angiogenesis and prognosis. *Clin Cancer Res* 9, 853-60.
28. Jackson, E. L., Willis, N., Mercer, K., Bronson, R. T., Crowley, D., Montoya, R., Jacks, T. & Tuveson, D. A. (2001). Analysis of lung tumor initiation and progression using conditional expression of oncogenic K-ras. *Genes Dev* 15, 3243-8.
29. Jackson, E. L., Olive, K. P., Tuveson, D. A., Bronson, R., Crowley, D., Brown, M. & Jacks, T. (2005). The differential effects of mutant p53 alleles on advanced murine lung cancer. *Cancer Res* 65, 10280-8.
30. Johnson, L., Mercer, K., Greenbaum, D., Bronson, R. T., Crowley, D., Tuveson, D. A. & Jacks, T. (2001). Somatic activation of the K-ras oncogene causes early onset lung cancer in mice. *Nature* 410, 1111-6.
31. Liu, G., McDonnell, T. J., Montes de Oca Luna, R., Kapoor, M., Mims, B., El-Naggar, A. K. & Lozano, G. (2000). High metastatic potential in mice inheriting a targeted p53 missense mutation. *Proc Natl Acad Sci U S A* 97, 4174-9.
32. Gibbons, D. L., Lin, W., Creighton, C. J., Zheng, S., Berel, D., Yang, Y., Raso, M. G., Liu, D. D., Wistuba, I., Lozano, G. & Kurie, J. M. (2009). Expression signatures of metastatic capacity in a genetic mouse model of lung adenocarcinoma. *PLoS One* 4, e5401.
33. Wislez, M., Fujimoto, N., Izzo, J. G., Hanna, A. E., Cody, D. D., Langley, R. R., Tang, H., Burdick, M. D., Sato, M., Minna, J. D., Mao, L., Wistuba, I., Strieter, R. M. & Kurie, J. M. (2006). High expression of ligands for chemokine receptor CXCR2 in alveolar epithelial neoplasia induced by oncogenic kras. *Cancer Res* 66, 4198-207.

34. Strieter, R. M., Burdick, M. D., Gomperts, B. N., Belperio, J. A. & Keane, M. P. (2005). CXC chemokines in angiogenesis. *Cytokine Growth Factor Rev* 16, 593-609.
35. Raghuwanshi, S. K., Nasser, M. W., Chen, X., Strieter, R. M. & Richardson, R. M. (2008). Depletion of beta-arrestin-2 promotes tumor growth and angiogenesis in a murine model of lung cancer. *J Immunol* 180, 5699-706.
36. Burger, M., Burger, J. A., Hoch, R. C., Oades, Z., Takamori, H. & Schraufstatter, I. U. (1999). Point mutation causing constitutive signaling of CXCR2 leads to transforming activity similar to Kaposi's sarcoma herpesvirus-G protein-coupled receptor. *J Immunol* 163, 2017-22.
37. Vandercappellen, J., Van Damme, J. & Struyf, S. (2008). The role of CXC chemokines and their receptors in cancer. *Cancer Lett* 267, 226-44.
38. Sun, H., Chung, W. C., Ryu, S. H., Ju, Z., Tran, H. T., Kim, E., Kurie, J. M. & Koo, J. S. (2008). Cyclic AMP-responsive element binding protein- and nuclear factor-kappaB-regulated CXC chemokine gene expression in lung carcinogenesis. *Cancer Prev Res (Phila)* 1, 316-28.
39. Yanagawa, J., Walser, T. C., Zhu, L. X., Hong, L., Fishbein, M. C., Mah, V., Chia, D., Goodglick, L., Elashoff, D. A., Luo, J., Magyar, C. E., Dohadwala, M., Lee, J. M., St John, M. A., Strieter, R. M., Sharma, S. & Dubinett, S. M. (2009). Snail promotes CXCR2 ligand-dependent tumor progression in non-small cell lung carcinoma. *Clin Cancer Res* 15, 6820-9.
40. Luppi, F., Longo, A. M., de Boer, W. I., Rabe, K. F. & Hiemstra, P. S. (2007). Interleukin-8 stimulates cell proliferation in non-small cell lung cancer through epidermal growth factor receptor transactivation. *Lung Cancer* 56, 25-33.
41. Maxwell, P. J., Gallagher, R., Seaton, A., Wilson, C., Scullin, P., Pettigrew, J., Stratford, I. J., Williams, K. J., Johnston, P. G. & Waugh, D. J. (2007). HIF-1 and

- NF-kappaB-mediated upregulation of CXCR1 and CXCR2 expression promotes cell survival in hypoxic prostate cancer cells. *Oncogene* 26, 7333-45.
42. Varney, M. L., Singh, S., Li, A., Mayer-Ezell, R., Bond, R. & Singh, R. K. (2010). Small molecule antagonists for CXCR2 and CXCR1 inhibit human colon cancer liver metastases. *Cancer Lett* 300, 180-8.
  43. Singh, S., Sadanandam, A., Nannuru, K. C., Varney, M. L., Mayer-Ezell, R., Bond, R. & Singh, R. K. (2009). Small-molecule antagonists for CXCR2 and CXCR1 inhibit human melanoma growth by decreasing tumor cell proliferation, survival, and angiogenesis. *Clin Cancer Res* 15, 2380-6.
  44. Johnson, Z., Power, C. A., Weiss, C., Rintelen, F., Ji, H., Ruckle, T., Camps, M., Wells, T. N., Schwarz, M. K., Proudfoot, A. E. & Rommel, C. (2004). Chemokine inhibition--why, when, where, which and how? *Biochem Soc Trans* 32, 366-77.
  45. White, J. R., Lee, J. M., Young, P. R., Hertzberg, R. P., Jurewicz, A. J., Chaikin, M. A., Widdowson, K., Foley, J. J., Martin, L. D., Griswold, D. E. & Sarau, H. M. (1998). Identification of a potent, selective non-peptide CXCR2 antagonist that inhibits interleukin-8-induced neutrophil migration. *J Biol Chem* 273, 10095-8.
  46. Gibbons, D. L., Lin, W., Creighton, C. J., Rizvi, Z. H., Gregory, P. A., Goodall, G. J., Thilaganathan, N., Du, L., Zhang, Y., Pertsemliadis, A. & Kurie, J. M. (2009). Contextual extracellular cues promote tumor cell EMT and metastasis by regulating miR-200 family expression. *Genes Dev* 23, 2140-51.
  47. Yang, Y., Ahn, Y. H., Gibbons, D. L., Zang, Y., Lin, W., Thilaganathan, N., Alvarez, C. A., Moreira, D. C., Creighton, C. J., Gregory, P. A., Goodall, G. J. & Kurie, J. M. (2011). The Notch ligand Jagged2 promotes lung adenocarcinoma metastasis through a miR-200-dependent pathway in mice. *J Clin Invest* 121, 1373-85.

48. Zheng, S., El-Naggar, A. K., Kim, E. S., Kurie, J. M. & Lozano, G. (2007). A genetic mouse model for metastatic lung cancer with gender differences in survival. *Oncogene* 26, 6896-904.
49. Yuan, P., Kadara, H., Behrens, C., Tang, X., Woods, D., Solis, L. M., Huang, J., Spinola, M., Dong, W., Yin, G., Fujimoto, J., Kim, E., Xie, Y., Girard, L., Moran, C., Hong, W. K., Minna, J. D. & Wistuba, II. (2010). Sex determining region Y-Box 2 (SOX2) is a potential cell-lineage gene highly expressed in the pathogenesis of squamous cell carcinomas of the lung. *PLoS One* 5, e9112.
50. Ijichi, H., Chytil, A., Gorska, A. E., Aakre, M. E., Bierie, B., Tada, M., Mohri, D., Miyabayashi, K., Asaoka, Y., Maeda, S., Ikenoue, T., Tateishi, K., Wright, C. V., Koike, K., Omata, M. & Moses, H. L. (2011). Inhibiting Cxcr2 disrupts tumor-stromal interactions and improves survival in a mouse model of pancreatic ductal adenocarcinoma. *J Clin Invest* 121, 4106-17.
51. Shedden, K., Taylor, J. M., Enkemann, S. A., Tsao, M. S., Yeatman, T. J., Gerald, W. L., Eschrich, S., Jurisica, I., Giordano, T. J., Misek, D. E., Chang, A. C., Zhu, C. Q., Strumpf, D., Hanash, S., Shepherd, F. A., Ding, K., Seymour, L., Naoki, K., Pennell, N., Weir, B., Verhaak, R., Ladd-Acosta, C., Golub, T., Gruidl, M., Sharma, A., Szoke, J., Zakowski, M., Rusch, V., Kris, M., Viale, A., Motoi, N., Travis, W., Conley, B., Seshan, V. E., Meyerson, M., Kuick, R., Dobbin, K. K., Lively, T., Jacobson, J. W. & Beer, D. G. (2008). Gene expression-based survival prediction in lung adenocarcinoma: a multi-site, blinded validation study. *Nat Med* 14, 822-7.
52. Lockwood, W. W., Chari, R., Coe, B. P., Girard, L., Macaulay, C., Lam, S., Gazdar, A. F., Minna, J. D. & Lam, W. L. (2008). DNA amplification is a ubiquitous mechanism of oncogene activation in lung and other cancers. *Oncogene* 27, 4615-24.

53. Zhou, B. B., Peyton, M., He, B., Liu, C., Girard, L., Caudler, E., Lo, Y., Baribaud, F., Mikami, I., Reguart, N., Yang, G., Li, Y., Yao, W., Vaddi, K., Gazdar, A. F., Friedman, S. M., Jablons, D. M., Newton, R. C., Fridman, J. S., Minna, J. D. & Scherle, P. A. (2006). Targeting ADAM-mediated ligand cleavage to inhibit HER3 and EGFR pathways in non-small cell lung cancer. *Cancer Cell* 10, 39-50.
54. Raponi, M., Zhang, Y., Yu, J., Chen, G., Lee, G., Taylor, J. M., Macdonald, J., Thomas, D., Moskaluk, C., Wang, Y. & Beer, D. G. (2006). Gene expression signatures for predicting prognosis of squamous cell and adenocarcinomas of the lung. *Cancer Res* 66, 7466-72.
55. Shames, D. S., Girard, L., Gao, B., Sato, M., Lewis, C. M., Shivapurkar, N., Jiang, A., Perou, C. M., Kim, Y. H., Pollack, J. R., Fong, K. M., Lam, C. L., Wong, M., Shyr, Y., Nanda, R., Olopade, O. I., Gerald, W., Euhus, D. M., Shay, J. W., Gazdar, A. F. & Minna, J. D. (2006). A genome-wide screen for promoter methylation in lung cancer identifies novel methylation markers for multiple malignancies. *PLoS Med* 3, e486.
56. Subramanian, A., Tamayo, P., Mootha, V. K., Mukherjee, S., Ebert, B. L., Gillette, M. A., Paulovich, A., Pomeroy, S. L., Golub, T. R., Lander, E. S. & Mesirov, J. P. (2005). Gene set enrichment analysis: a knowledge-based approach for interpreting genome-wide expression profiles. *Proc Natl Acad Sci U S A* 102, 15545-50.
57. Onn, A., Isobe, T., Itasaka, S., Wu, W., O'Reilly, M. S., Ki Hong, W., Fidler, I. J. & Herbst, R. S. (2003). Development of an orthotopic model to study the biology and therapy of primary human lung cancer in nude mice. *Clin Cancer Res* 9, 5532-9.
58. Roybal, J. D., Zang, Y., Ahn, Y. H., Yang, Y., Gibbons, D. L., Baird, B. N., Alvarez, C., Thilaganathan, N., Liu, D. D., Saintigny, P., Heymach, J. V.,



- Creighton, C. J. & Kurie, J. M. (2011). miR-200 Inhibits lung adenocarcinoma cell invasion and metastasis by targeting Flt1/VEGFR1. *Mol Cancer Res* 9, 25-35.
59. Singh, S., Varney, M. & Singh, R. K. (2009). Host CXCR2-dependent regulation of melanoma growth, angiogenesis, and experimental lung metastasis. *Cancer Res* 69, 411-5.
60. Murphy, C., McGurk, M., Pettigrew, J., Santinelli, A., Mazzucchelli, R., Johnston, P. G., Montironi, R. & Waugh, D. J. (2005). Nonapical and cytoplasmic expression of interleukin-8, CXCR1, and CXCR2 correlates with cell proliferation and microvessel density in prostate cancer. *Clin Cancer Res* 11, 4117-27.
61. Wang, B., Hendricks, D. T., Wamunyokoli, F. & Parker, M. I. (2006). A growth-related oncogene/CXC chemokine receptor 2 autocrine loop contributes to cellular proliferation in esophageal cancer. *Cancer Res* 66, 3071-7.
62. Yang, G., Rosen, D. G., Liu, G., Yang, F., Guo, X., Xiao, X., Xue, F., Mercado-Uribe, I., Huang, J., Lin, S. H., Mills, G. B. & Liu, J. (2010). CXCR2 promotes ovarian cancer growth through dysregulated cell cycle, diminished apoptosis, and enhanced angiogenesis. *Clin Cancer Res* 16, 3875-86.
63. Fan, G. H., Lapierre, L. A., Goldenring, J. R. & Richmond, A. (2003). Differential regulation of CXCR2 trafficking by Rab GTPases. *Blood* 101, 2115-24.
64. Kuo, P. L., Chen, Y. H., Chen, T. C., Shen, K. H. & Hsu, Y. L. (2010). CXCL5/ENA78 increased cell migration and epithelial-to-mesenchymal transition of hormone-independent prostate cancer by early growth response-1 /Snail signaling pathway. *J Cell Physiol*.
65. Ohri, C. M., Shikotra, A., Green, R. H., Waller, D. A. & Bradding, P. (2010). Chemokine receptor expression in tumour islets and stroma in non-small cell lung cancer. *BMC Cancer* 10, 172.

66. Acosta, J. C., O'Loghlen, A., Banito, A., Guijarro, M. V., Augert, A., Raguz, S., Fumagalli, M., Da Costa, M., Brown, C., Popov, N., Takatsu, Y., Melamed, J., d'Adda di Fagagna, F., Bernard, D., Hernando, E. & Gil, J. (2008). Chemokine signaling via the CXCR2 receptor reinforces senescence. *Cell* 133, 1006-18.
67. Roussos, E. T., Keckesova, Z., Haley, J. D., Epstein, D. M., Weinberg, R. A. & Condeelis, J. S. (2010). AACR special conference on epithelial-mesenchymal transition and cancer progression and treatment. *Cancer Res* 70, 7360-4.
68. Tang, X., Kadara, H., Behrens, C., Liu, D. D., Xiao, Y., Rice, D., Gazdar, A. F., Fujimoto, J., Moran, C., Varella-Garcia, M., Lee, J. J., Hong, W. K. & Wistuba, II. (2011). Abnormalities of the TTF-1 lineage-specific oncogene in NSCLC: implications in lung cancer pathogenesis and prognosis. *Clin Cancer Res* 17, 2434-43.
69. Massarelli, E., Varella-Garcia, M., Tang, X., Xavier, A. C., Ozburn, N. C., Liu, D. D., Bekele, B. N., Herbst, R. S. & Wistuba, II. (2007). KRAS mutation is an important predictor of resistance to therapy with epidermal growth factor receptor tyrosine kinase inhibitors in non-small-cell lung cancer. *Clin Cancer Res* 13, 2890-6.
70. Miyazaki, H., Patel, V., Wang, H., Edmunds, R. K., Gutkind, J. S. & Yeudall, W. A. (2006). Down-regulation of CXCL5 inhibits squamous carcinogenesis. *Cancer Res* 66, 4279-84.
71. Speetjens, F. M., Kuppen, P. J., Sandel, M. H., Menon, A. G., Burg, D., van de Velde, C. J., Tollenaar, R. A., de Bont, H. J. & Nagelkerke, J. F. (2008). Disrupted expression of CXCL5 in colorectal cancer is associated with rapid tumor formation in rats and poor prognosis in patients. *Clin Cancer Res* 14, 2276-84.

72. Tessema, M., Klinge, D. M., Yingling, C. M., Do, K., Van Neste, L. & Belinsky, S. A. (2010). Re-expression of CXCL14, a common target for epigenetic silencing in lung cancer, induces tumor necrosis. *Oncogene* 29, 5159-70.
73. Peng, W., Ye, Y., Rabinovich, B. A., Liu, C., Lou, Y., Zhang, M., Whittington, M., Yang, Y., Overwijk, W. W., Lizee, G. & Hwu, P. (2010). Transduction of tumor-specific T cells with CXCR2 chemokine receptor improves migration to tumor and antitumor immune responses. *Clin Cancer Res* 16, 5458-68.

## VITA

Erminia Massarelli was born in Naples, Italy on November 27, 1972, the daughter of Cristina Avolio and Luigi Massarelli. After completing her work at Giuseppe Garibaldi high school, Naples, Italy, she entered Medical School at the University of Naples Federico II, Naples, Italy. She received her medical school degree with summa cum laude on July 22, 1997. She then entered the Specialization in Medical Oncology at the University of Naples Federico II, and completed her clinical training in October 2001, passing the Italian Board of Medical Oncology in October 2001. She entered her PhD in Molecular Oncology and Endocrinology in November 2001 at the University of Naples Federico II, Naples, Italy where she was included in an international program that allowed her to spend the last two years of her research training at MD Anderson Cancer Center, Houston, Texas. She received her PhD degree in February 2006. She also completed her postdoctoral fellowship in the Department of Thoracic Head and Neck Medical Oncology at MD Anderson Cancer Center, Houston, Texas in July 2007. She then enrolled into the Internal Medicine Residency program at the Methodist Hospital, Houston Texas and completed her training in July 2009. Dr. Massarelli passed the ABIM board certification in Internal Medicine in August 2010. Subsequently she entered the clinical Medical Oncology Fellowship program at MD Anderson Cancer Center, Houston, Texas in July 2009 and completed her clinical training in July 2012. In August 2011 she entered The University of Texas Health Science Center at Houston Graduate School of Biomedical Sciences. Dr. Massarelli passed the ABIM board certification in Medical Oncology in October 2012. Since November 2012 she holds an Assistant Professor position in the Department of Thoracic Head and Neck Medical Oncology at MD Anderson Cancer Center, Houston, Texas.